CHEMISTRY
A European Journal

A Journal of
ChemPubSoc Europe

Accepted Article

Title: On the redox reactivity of a geometrically constrained phosphorus(III) compound.

Authors: Thomas Robinson, Daniel De Rosa, Simon Aldridge, and Jose Manuel Goicoechea

To be cited as: *Chem. Eur. J.* 10.1002/chem.201703119

Link to VoR: http://dx.doi.org/10.1002/chem.201703119

Supported by
ACES

WILEY-VCH

10.1002/chem.201703119

On the redox reactivity of a geometrically constrained phosphorus(III) compound.

Thomas P. Robinson, Daniel De Rosa, Simon Aldridge and Jose M. Goicoechea*

Department of Chemistry, University of Oxford, Chemistry Research Laboratory, 12 Mansfield Road, Oxford, OX1 3TA, U.K.

E-mail: jose.goicoechea@chem.ox.ac.uk

Abstract

The reactivity of a geometrically constrained phosphorus(III) complex bearing the *N*,*N*-bis(3,5-di-*tert*-butyl-2-phenolate)amide pincer ligand (P(ONO); **1**) towards oxidants and reductants is explored. This compound can be readily oxidized to the phosphorus(V) dihalo-derivatives P(ONO)X_2 where X = Cl (**2**), Br (**3**) and I (**4**). Attempts at isolating the analogous difluoride through oxidation of **1** were unsuccessful yielding only the hydrofluoride P(ONO)(H)F (**5**), however P(ONO)F_2 (**6**) can be accessed via a halide exchange reaction of **2** with KF. Compound **2** can be employed as a precursor to novel cationic species through chloride ion displacement using strong Lewis bases. Thus, reaction of **2** with two or three molar equivalents of dimethylaminopyridine (DMAP) affords $[P(ONO)(Cl)(DMAP)_2]^+$ (**7**) and $[P(ONO)(DMAP)_3]^{2+}$ (**8**). Reaction of **2** with the weaker bidentate base 2,2′-bipyridine (bipy) affords $[P(ONO)(Cl)(bipy)]^+$ (**9**), although this species was only accessible upon addition of a halide abstracting agent. The dicationic tris(pyridine) adduct $[P(ONO)(py)_3]^{2+}$ (**10**) is also accessible by reaction of **4** with pyridine. Oxidation of **1** using oxygen gas proceeds slowly and allows for the observation of two compounds, a mixed valence dimeric phosphorus(III)/phosphorus(V) compound $[P(ONO)(\mu^2\text{-}O)(\mu^2\text{:}\kappa^1,\kappa^2\text{-}ONO)P]$ (**11**) and the fully oxidized species $[P(ONO)(\mu^2\text{-}O)(\mu^2\text{:}\kappa^1,\kappa^2\text{-}ONO)P(O)]$ (**12**). Finally, reaction of **1** using KC_8 results in the dimerization of the putative radical anion $[P(ONO)]^{\cdot-}$ through formation of

a P–P bond to afford $[P(ONO)]_2^{2-}$ (**13**). Reactions with TEMPO result in the formation of the trigonal bipyramidal species $P(ONO)(TEMPO)_2$ (**14**).

1. Introduction

Geometrically constrained phosphorus(III) compounds have recently received significant attention following studies demonstrating that such species are capable of activating small molecule substrates including ammonia, amines, water, alcohols and ammonia–borane. Studies by Arduengo,[1] Radosevich,[2–4] Kinjo,[5] and our own research group,[6] have demonstrated that the distorted T-shaped phosphorus(III) compounds pictured in Figure 1 are capable of undergoing formal oxidative addition reactions to afford trigonal bipyramidal phosphorus(V) compounds. The reactivity of such species towards common nucleophiles and electrophiles seems to highlight that such reactions are unlikely to proceed in a concerted fashion at the phosphorus centre, but rather that the ligand framework is intimately involved in such reactions.[7,8] Several theoretical studies have also corroborated this hypothesis.[9,10]

This class of compounds forms part of a rapidly increasing family of main group element-containing species that have been shown to activate small molecule substrates,[11] the most notable of which are alkyl(amino) carbenes (AACs),[12] low oxidation state compounds of the triel and tetrel elements,[13,14] and frustrated Lewis pairs (FLPs).[15] A number of such species have even been shown to be active in catalytic processes, such as the hydrogenation of imines, alkenes, alkynes, aldehydes and ketones,[16] making the prospect of carrying out catalytic transformations using elements with a high crustal abundance an increasingly attractive target.

10.1002/chem.201703119

Given the importance of ligand framework in the reactivity of the compounds pictured in Scheme 1, we were intrigued to establish whether the known redox active ligand *N*,*N*-bis(3,5-di-*tert*-butyl-2-phenolate)amide ligand present in **1**,[17] had any involvement in the reactivity of this species towards common oxidants and reductants. The results of our studies are reported herein.

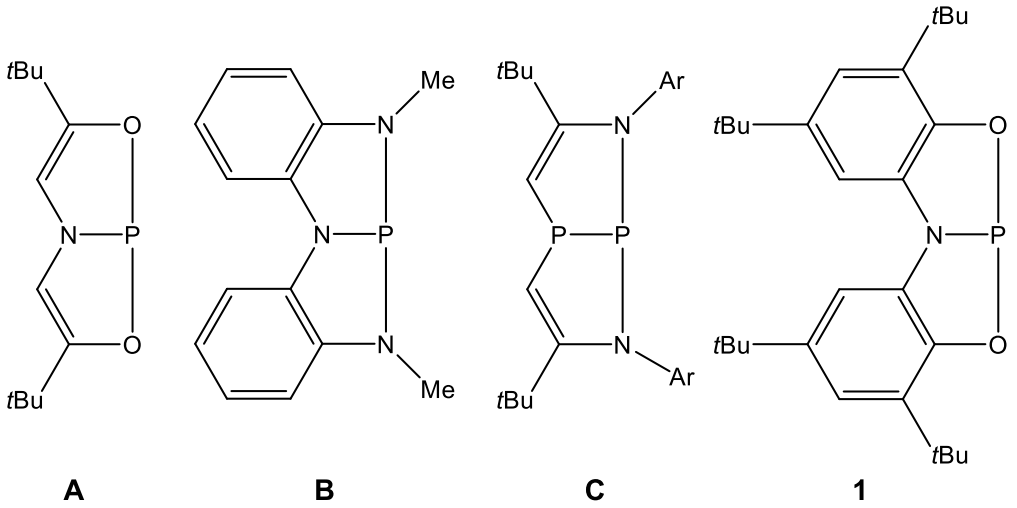

Figure 1. Selected geometrically constrained phosphorus(III) compounds capable of activating small molecules (Ar = 2,6-diisopropylphenyl).

2. Results and discussion

*2.1. Oxidation of **1** to afford phosphorus(V) dihalo-derivatives*

In order to investigate the chemical oxidation chemistry of **1** mediated by non-nucleophilic substrates its reactivity towards elemental halogens was probed. For both chlorine and bromine, PX_5 (X = Cl or Br) was used as an *in situ* source of X_2, whilst elemental iodine could be used directly. All of these reactions generated the dihalide compounds $P(ONO)X_2$ where X = Cl (**2**), Br (**3**) and I (**4**). It should be noted that **2** was first reported by Contreras and co-workers and was recently employed by Radosevich for the synthesis of phosphorane based radicals.[18,19] Upon dissolving the two reagents in toluene full consumption of **1** was observed by ^{31}P NMR spectroscopy and the formation of the respective phosphorus(V)

10.1002/chem.201703119

dihalides was indicated by singlet resonances at −21.0 (**2**), −88.2 (**3**) and −258.3 ppm (**4**). The NMR data for **2** and **3** are in good agreement with other related phosphorus(V) dihalides previously reported by Arduengo.[1,20]. All of the dihalides were isolated as crystalline samples from concentrated toluene solutions and were colourless, yellow, and dark red for **2**, **3**, and **4**, respectively. The identity of each product was confirmed by single crystal X-ray diffraction studies (Figure 2). The five-coordinate phosphorus centres tend towards square-based pyramidal geometries, increasingly so for the heavier halides (τ = 0.40 (**2**), 0.33 (**3**) and 0.24 (**4**),[21] with one halide occupying the pseudo-axial position. This is reflected by a shorter P–X_{axial} bond and a longer P–X_{basal} bond within each compound. For example, in the case of **4**, the P–I_{axial} bond is 2.464(1) Å compared to the P–I_{basal} bond of 2.501(1) Å. The P–N bond lengths for all three compounds are identical within experimental error 1.696(1), 1.702(4) and 1.700(3) Å for **2**–**4**, respectively. The same is also true of the P–O bonds: 1.667(1) and 1.667(1) for **2**, 1.661(3) and 1.663(3) for **3** and 1.672(2) and 1.670(2) Å for **4**.

10.1002/chem.201703119

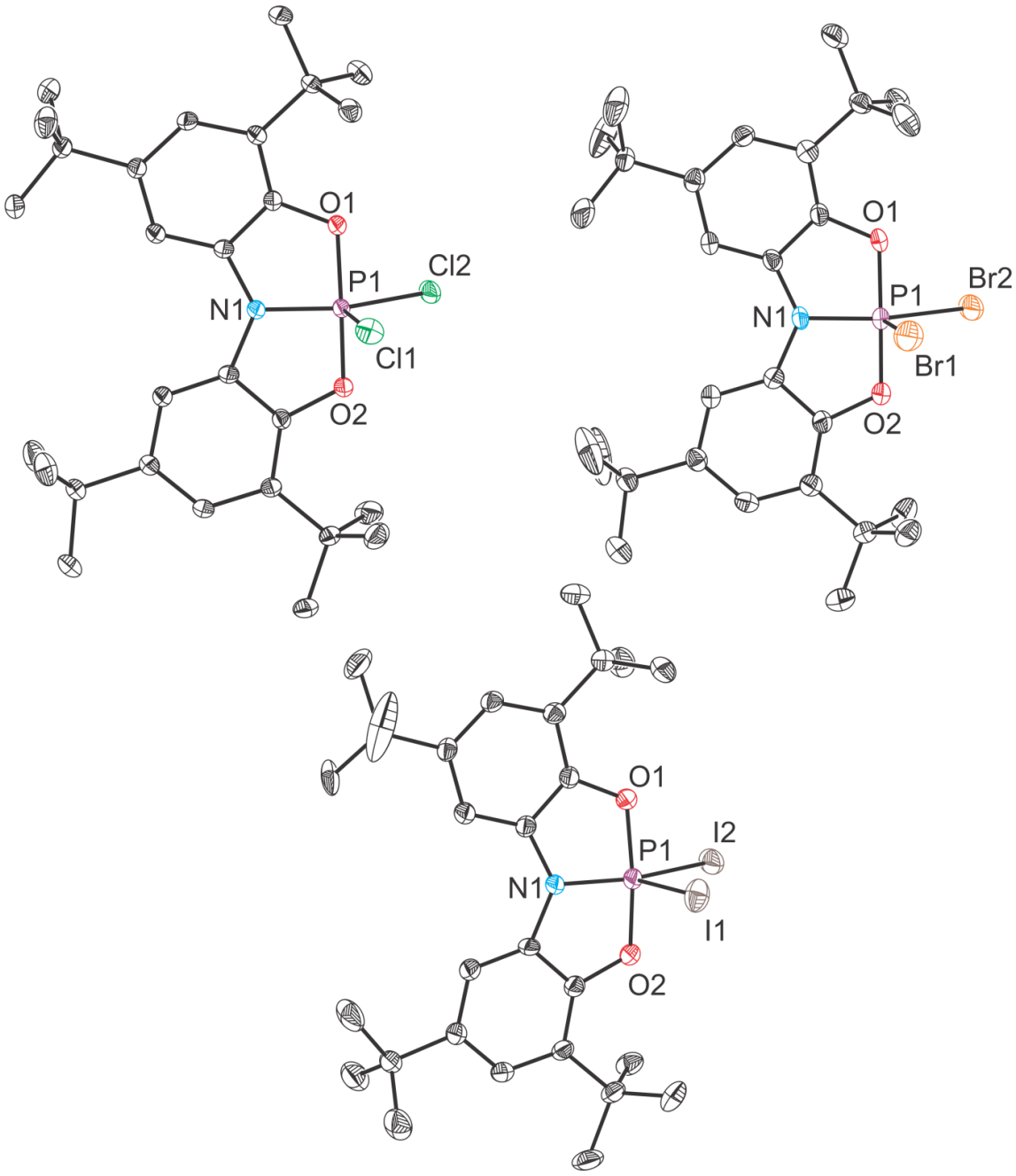

Figure 2. Molecular structures of $P(ONO)X_2$ where X = Cl (**2**), Br (**3**) or I (**4**). Thermal ellipsoids set at 50% probability; hydrogen atoms and solvent of crystallisation are omitted for clarity. Selected bond lengths [Å] and angles [°]: **2**: P1–N1 1.696(1), P1–O1 1.667(1), P1–O2 1.667(1), P1–Cl1 2.038(1), P1–Cl2 2.047(1); O1–P1–O2 167.91(5), O1–P1–N1 88.86(4), O1–P1–Cl1 95.71(4), O1–P1–Cl2 87.52(3), O2–P1–N1 88.71(4), O2–P1–Cl1 96.21(4), O2–P1–Cl2 87.49(4), N1–P1–Cl1 111.11(4), N1–P1–Cl2 143.98(4), Cl1–P1–Cl2 104.91(2). **3**: P1–N1 1.702(4), P1–O1 1.661(3), P1–O2 1.663(3), P1–Br1 2.219(2), P1–Br

2.235(2); O1–P1–O2 165.42(19), O1–P1–N1 88.51(17), O1–P1–Br1 96.98(13), O1–P1–Br2 86.40(12), O2–P1–N1 89.94(18), O2–P1–Br1 97.29(14), O2–P1–Br2 86.82(12), N1–P1–Br1 107.88(15), N1–P1–Br2 146.11(16), Br1–P1–Br2 105.99(5). **4**: P1–N1 1.700(3), P1–O1 1.672(2), P1–O2 1.670(2), P1–I1 2.464(1), P1–I2 2.501(1); O1–P1–O2 162.77(14), O1–P1–N1 89.07(12), O1–P1–I1 98.92(10), O1–P1–I2 86.32(9), O2–P1–N1 89.31(12), O2–P1–I1 98.00(9), O2–P1–I2 85.95(9), N1–P1–I1 106.30(11), N1–P1–I2 147.86(11), I1–P1–I2 105.84(3).

Compound **3** represents a very rare example of a phosphorus(V) dibromide with previous examples relying on either arylimino or highly electron withdrawing fluoroaryl substituents.[22] Furthermore, to the best of our knowledge, **4** represents the first structurally characterised example of a phosphorus(V) diiodide with other species of the formula R_3PI_2 shown to adopt either phosphonium iodides or "spoke" charge-transfer adducts.[23] It is noteworthy that the extremely upfield ^{31}P NMR chemical shift associated with **4** suggests that the five-coordinate structure persists in solution. Examples of phosphorus(V) monoiodides are also scarce, again requiring arylimino moieties.[24] These observations evidence the low oxidation potential of **1**, supporting the facility of small molecule activation at the phosphorus(III) centre.

The synthesis of the analogous difluoride compound, $P(ONO)F_2$, has also been investigated, using xenon difluoride as a source of F_2. When this reaction is performed in deuterated dichloromethane the solution turns black immediately and ^{31}P NMR spectroscopy reveals a 2:1 product mixture, with a doublet of doublets resonance centred at −31.9 ppm and a triplet resonance centred at –38.1 ppm, respectively. The former collapses to a doublet upon proton decoupling. Complementary $^1J_{F–P}$ coupling constants are observed in the ^{19}F NMR spectrum

($^1J_{F–P}$ = 872 and 1047 Hz, respectively). The NMR spectral data suggests the formation of both the targeted phosphorus difluoride (the species observed at 38.1 ppm) and also the hydrofluoride, P(ONO)(H)F (**5**), which is formed as the major product. The related hydrochloride complex has been recently reported by our research group and exhibits an almost identical ^{31}P NMR chemical shift (−31.3 ppm). The origin of the hydride in this complex is unclear although the absence of deuteride rules out the reaction solvent and thus suggests abstraction from **1**. When the same reaction is performed in toluene, we observe almost exclusive formation of the hydrofluoride product. Crystals of this species were grown from a concentrated hexane solution (Figure 3, left).

Given the difficulties associated with direct fluorination of **1**, the difluoride compound, $P(ONO)F_2$ (**6**), was targeted by treatment of dichloride **2** with a stoichiometric excess of KF. The ^{31}P NMR spectrum of a C_6D_6 solution of **6** revealed a triplet at −38.2 ppm with a $^1J_{P–F}$ coupling constant of 879 Hz. A doublet resonance with the same coupling constant was observed in the ^{19}F NMR spectrum at −55.7 ppm. Compositionally pure crystals of **6** suitable for single crystal X-ray diffraction were obtained by cooling hexane solutions of the product to –30 °C. The crystal structure of **6** (Figure 3, right) is very similar those previously reported for **2**–**4** with P–O bond lengths of 1.655(2) and 1.650(2) Å and a P–N bond length of 1.681(3) Å (cf. 1.696(1), 1.702(4) and 1.700(3) for **2**–**4**, respectively). The P–X bond distances on going from F to I increase in accordance with the increase in covalent radius of the halogens (P–X where X = F: 1.635(3); Cl: 2.043 (av); Br: 2.227 (av); I: 2.483 (av) Å). Compound **6** crystallizes in the orthorhombic space group $Cmc2_1$, with the *N*,*N*-bis(3,5-di-*tert*-butyl-2-phenolate)amide lying on a crystallographic mirror plane, consequently both fluoride ligands are related by symmetry. This makes the determination of the τ parameter for **6** somewhat artificial as the high symmetry may mask some positional disorder of the

10.1002/chem.201703119

fluorine atoms. Regardless, the calculated τ value for **6** is 0.85 which makes it the most trigonal bipyramidal compound of the series, fitting in with the trend observed for the heavier halogen analogues (*vide supra*).

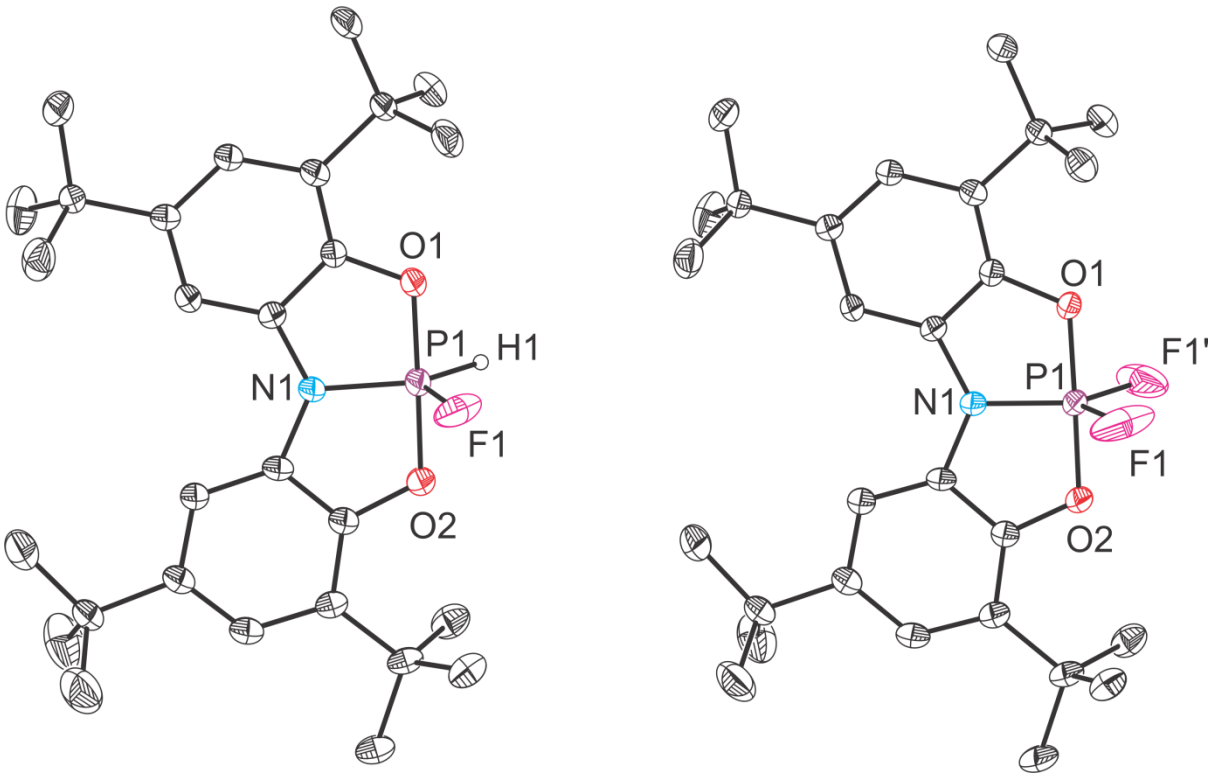

Figure 3. Molecular structures of P(ONO)(H)(F) (**5**; left) and P(ONO)F_2 (**6**; right). Thermal ellipsoids set at 50% probability; hydrogen atoms, with the exception of H1 in **5** and any disordered component omitted for clarity. Selected bond lengths [Å] and angles [°]: **5**: P1–N1 1.689(3), P1–O1 1.663(2), P1–O2 1.654(2), P1–F1 1.635(3), P1–H1 1.36(2); O1–P1–O2 179.13(12), O1–P1–N1 89.54(12), O1–P1–F1 90.11(10), O1–P1–H1 89.6(7), O2–P1–N1 89.59(11), O2–P1–F1 90.13(10), O2–P1–H1 91.0(7), N1–P1–F1 106.30(15), N1–P1–H1 141.5(17), F1–P1–H1 112.2(18). **6**: P1–N1 1.681(3), P1–O1 1.655(2) P1–O2 1.650(2), 1.538(2); O1–P1–O2 179.05(11), O1–P1–N1 89.51(11), O1–P1–F1 90.25(8), O2–P1–N1 89.53(11), O2–P1–F1 90.34(8), N1–P1–F1 128.00(11), F1–P1–F1' 104.0(2). Symmetry operation ′: 2–*x*, +*y*, +*z*.

10.1002/chem.201703119

2.2. Halide ion displacement from P(ONO)X$_2$

When studying the aforementioned compounds, it became apparent that they are relatively unstable in strong donor solvents. This prompted us to explore the reactivity of **2**–**4** towards Lewis basic substrates. Addition of two equivalents of dimethylaminopyridine (DMAP) to a dichloromethane solution of **2** results in displacement of one of the chloride substituents and coordination of both molecules of DMAP to the phosphorus centre. The ^{31}P NMR spectrum of the resulting cation reveals a single broad resonance at −102.0 ppm whilst the ^{1}H NMR spectrum shows sharp resonances attributed to the aryl and *tert*-butyl environments of the ligand, in addition to broad resonances at 8.69, 7.78, 6.66 and 3.22 ppm corresponding to fluxional DMAP moieties. Upon cooling solutions to −50 °C, both ^{31}P and ^{1}H NMR resonances sharpen with the latter showing two distinct DMAP environments. Crystals of the product, [P(ONO)(DMAP)$_2$Cl]Cl ([**7**]Cl), were grown by slow diffusion of hexane into the dichloromethane reaction mixture. Single crystal X-ray diffraction studies reveal a bis-DMAP adduct of [P(ONO)Cl]$^+$ in which the phosphorus centre exhibits an octahedral geometry (Figure 4). The ONO^{3-} ligand adopts a meridional coordination mode and the DMAP ligands are *cis* and *trans* to the chloride, supporting the observation of two distinct DMAP environments in the low temperature ^{1}H NMR spectrum. The DMAP ligands both coordinate through the pyridine nitrogen atom and the P–N$_{DMAP}$ bond lengths (1.846(2) and 1.867(2) Å) are slightly longer than Σr_{cov}(P–N) (1.82 Å).[25] This suggests relatively weak coordination of these ligands whilst the slightly longer P1–N4 bond reflects the greater *trans* influence of the chloride relative to the amide donor. On coordination of the two DMAP molecules the P–Cl bond increases significantly to 2.270(1) Å, relative to those observed in the dichloride precursor **2** (2.038(1), and 2.047(1) Å).

10.1002/chem.201703119

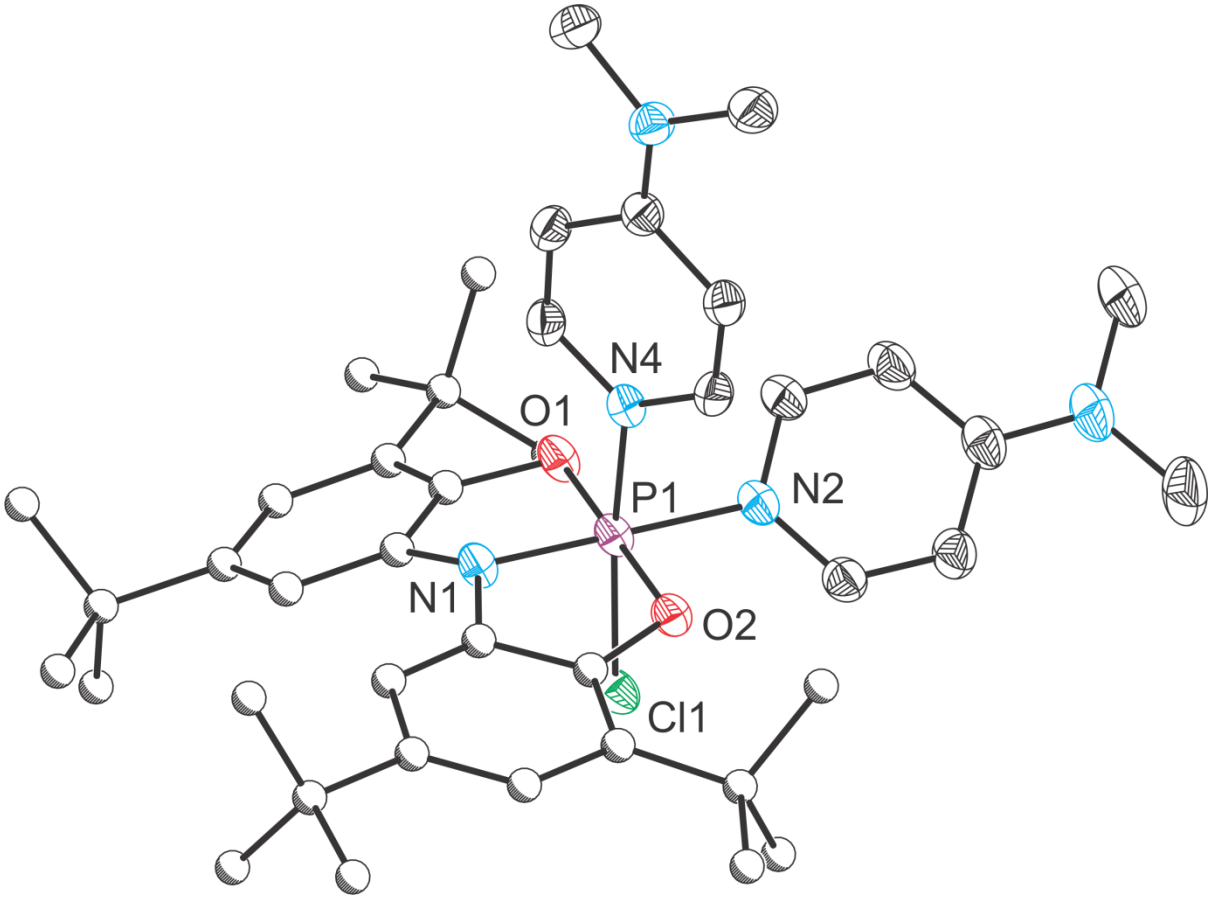

Figure 4. Structure of $[P(ONO)(Cl)(DMAP)_2]^+$ (**7**). Thermal ellipsoids set at 50% probability; hydrogen atoms, solvent of crystallisation and chloride counter anion are omitted for clarity. Selected bond lengths [Å] and angles [°]: P1–N1 1.733(2), P1–N2 1.846(2), P1–N4 1.867(2), P1–O1 1.662(2), P1–O2 1.662(2), P1–Cl1 2.270(1); O1–P1–O2 177.81(7), O1–P1–N1 91.34(7), O1–P1–N2 89.10(7), O1–P1–N4 90.63(7), O1–P1–Cl1 88.46(5), O2–P1–N1 89.77(7), O2–P1–N2 89.79(7), O2–P1–N4 91.21(7), O2–P1–Cl1 89.61(5), N1–P1–N2 179.52(8), N1–P1–N4 92.73(7), N1–P1–Cl1 92.18(6), N2–P1–N4 87.44(7), N2–P1–Cl1 87.65(5), N4–P1–Cl1 175.02(5).

Addition of a further equivalent of DMAP results in displacement of the second chloride substituent to yield a tris-DMAP adduct of $[P(ONO)]^{2+}$, $[P(ONO)(DMAP)_3]Cl_2$ ([**8**][Cl]$_2$), exhibiting a broad ^{31}P NMR resonance at −117.0 ppm. Performing the reaction in chloroform results in the precipitation of colourless crystals, however, the product crystallises with a

10.1002/chem.201703119

large amount of solvent in the lattice, which has precluded the collection of a high quality X-ray diffraction data set, although the connectivity observed supports the formation of the expected product (Figure 5). The product is also evidenced by elemental analyses consistent with the expected formula. Repeated attempts to dissolve crystals of **8** in $CDCl_3$ result in partial decomposition to the monocation **7** and DMAP hydrochloride.

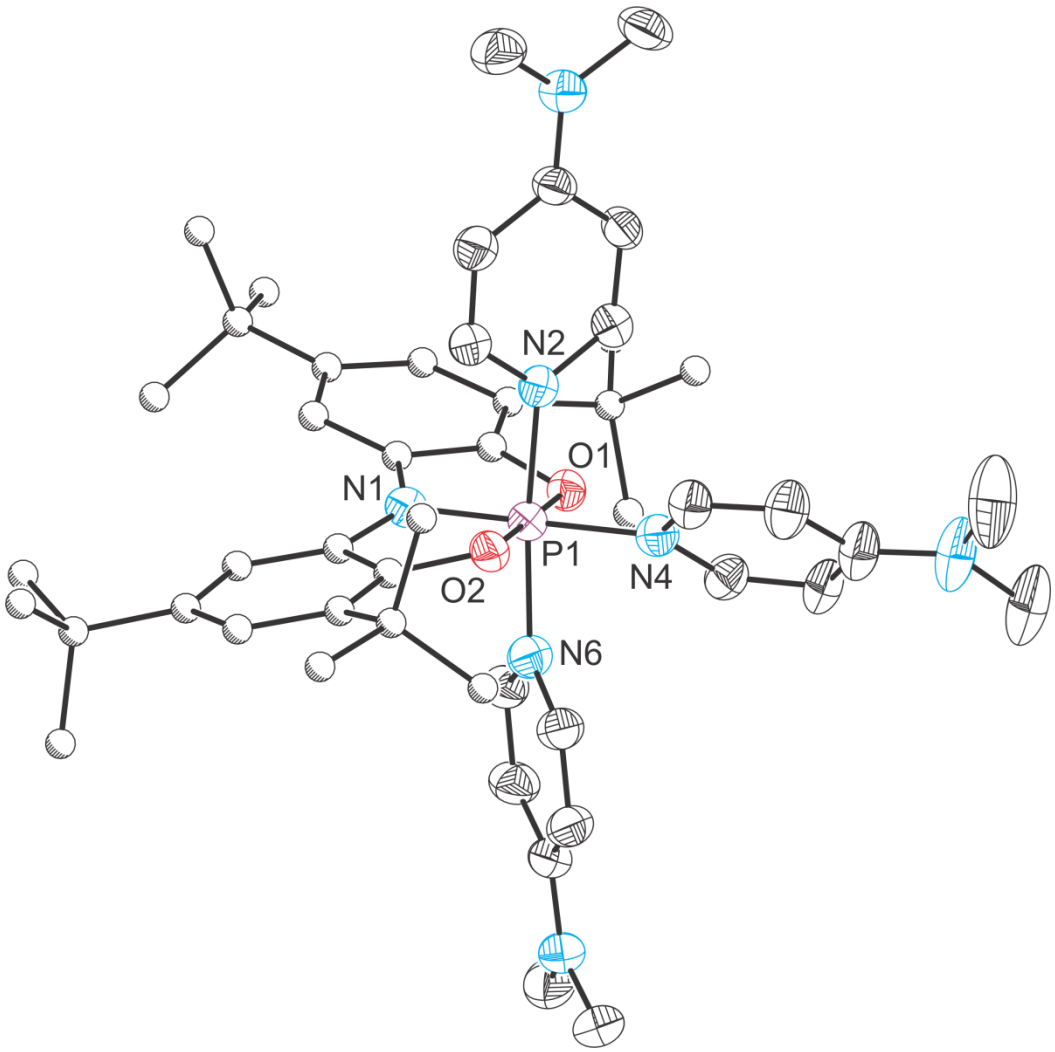

Figure 5. Structure of $[P(ONO)(DMAP)_3]^{2+}$ (**8**). Thermal ellipsoids set at 50% probability; hydrogen atoms, solvent of crystallisation and chloride counter anions are omitted for clarity. Selected bond lengths [Å] and angles [°]: P1–N1 1.720(4), P1–N2 1.897(3), P1–N4 1.833(4), P1–N6 1.884(3), P1–O1 1.666(2), P1–O2 1.667(2); O1–P1–O2 179.37(15), O1–P1–N1 90.03(14), O1–P1–N2 89.56(12), O1–P1–N4 89.51(13), O1–P1–N6 90.26(13), O2–P1–N1 90.32(15), O2–P1–N2 89.89(12), O2–P1–N4 90.14(13), O2–P1–N6 90.26(13), N1–P1–N2

92.82(15), N1–P1–N4 179.45(15), N1–P1–N6 92.76(15), N2–P1–N4 86.87(14), N2–P1–N6 174.43(16), N4–P1–N6 87.55(15).

Compound **8**, displays an octahedral geometry with the *N*,*N*-bis(3,5-di-*tert*-butyl-2-phenolate)amide ligand in a meridional coordination environment. The two DMAP ligands *trans* to one another exhibit notably longer P–N bond lengths (1.897(3), 1.884(3) Å), than that of the DMAP ligand *trans* to the amide position of the ONO^{3-} ligand (1.833(4) Å). This is consistent with the greater *trans*-influence of the DMAP substituents and its decreased π-acceptor properties relative to the ONO^{3-} amide. The former P–N bond lengths are long for single bonds and are indicative that there is only a very weak interaction between these ligands and the phosphorus centre.

By reducing the polarity of the solvent used to prepare the dication an equilibrium between **7** and **8** can be observed in solution. Using three equivalents of DMAP and one equivalent of **2** in CD_2Cl_2, the room temperature ^{31}P NMR spectrum shows two broad resonances reflecting an approximate 1:1 mixture of [**7**]Cl and [**8**][Cl]$_2$. The respective ^{1}H NMR spectrum shows a series of broad resonances corresponding to the exchanging DMAP ligands, the ONO^{3-} ligand backbone and one of the ^{t}Bu environments. Upon cooling, the amount of [**8**][Cl]$_2$ in solution increases until, at −50 °C, it is the only species present with both ^{1}H and ^{31}P NMR spectra exhibiting only sharp resonances. It is noteworthy that, although full conversion to **8** is observed in $CDCl_3$, lability of the DMAP ligands can be seen upon heating such solutions; at 50 °C the ^{31}P NMR spectrum shows two broad resonances corresponding to **7** and **8** with an integral ratio of 1:1.6.

10.1002/chem.201703119

Surprisingly, other Lewis bases such isocyanides and phosphines do not react with **2**, even when heated. Furthermore, 2,2-bipyridine, a unimolecular (albeit slightly less strongly donating) model of the two DMAP ligands also fails to displace a chloride from **2**, although the reaction can be promoted by adding an equivalent of a chloride abstracting agent such as Na[BAr^F_4] to deliver green solutions of cation **9**, which exhibits a singlet resonance at −77.2 ppm. Layering concentrated dichloromethane solutions of [**9**][BAr^F_4] with hexane affords large crystals of the product and the structure could then be confirmed by subsequent X-ray diffraction studies (Figure 6). In analogy to the structure of **7**, the phosphorus centre exhibits an octahedral geometry, with the chloride substituent sitting perpendicular to the planar pincer ligand. The P–N bonds to the bipy ligand (1.901(2), 1.957(2) Å) are significantly longer than the analogous P–N_{DMAP} bonds of **7**, consistent with the weaker Lewis basicity of the former. It is likely to be for this reason that Na[BAr^F_4] is required to facilitate the reaction. The reduced donation of electron density is compensated for by the shorter P–O and P–N to the ligand and a shorter P–Cl bond in **9**.

10.1002/chem.201703119

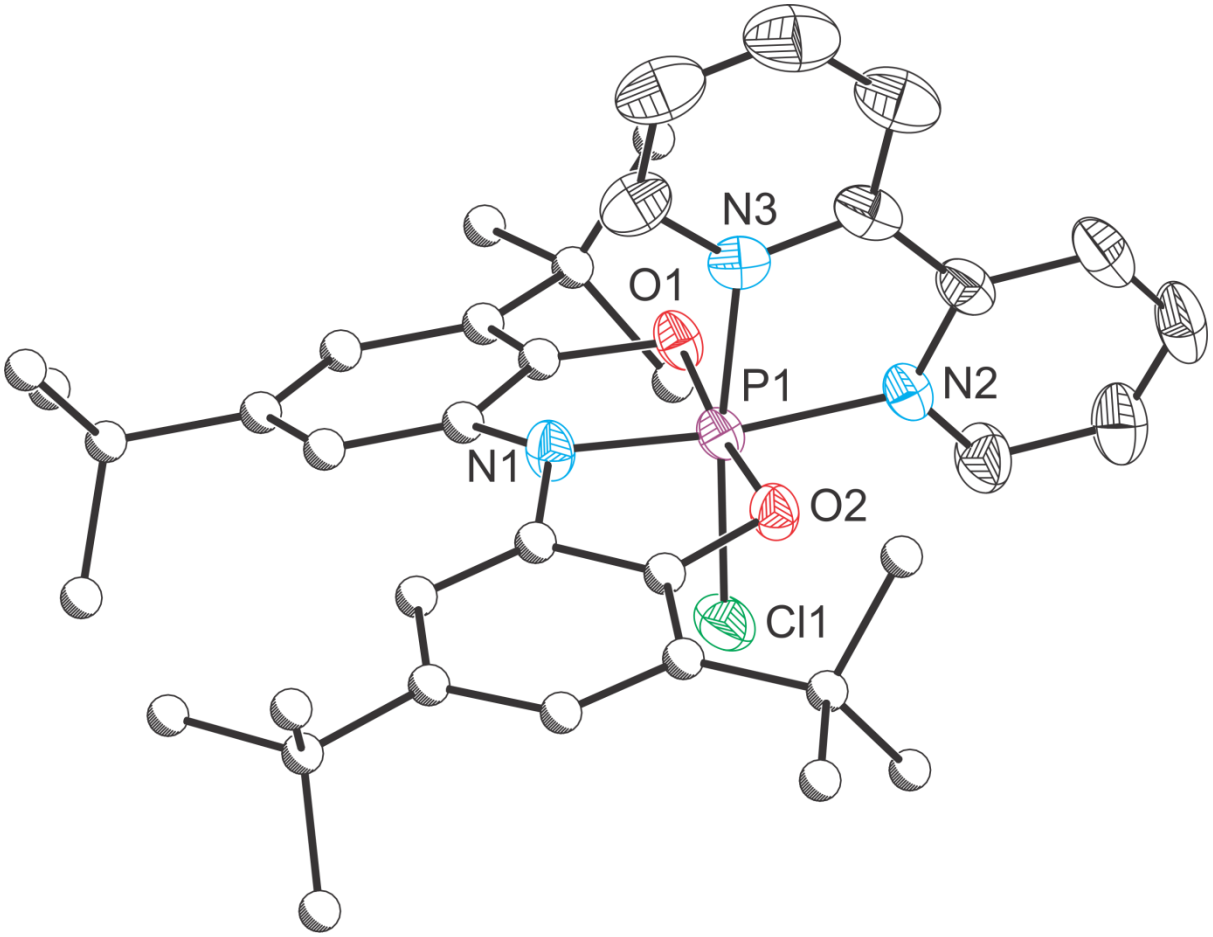

Figure 6. Structure of $[P(ONO)(Cl)(bipy)]^+$ (**9**). Thermal ellipsoids set at 50% probability; hydrogen atoms and $[BAr^F{}_4]^-$ counter anion are omitted for clarity. Selected bond lengths [Å] and angles [°]: P1–N1 1.714(2), P1–O1 1.651(2), P1–O2 1.656(2), P1–Cl1 2.137(1), P1–N2 1.901(2), P1–N3 1.957(2); O1–P1–O2 173.28(8), O1–P1–N1 92.51(8), O1–P1–Cl1 94.19(7), O1–P1–N2 88.35(8), O1–P1–N3 85.41(8), O2–P1–N1 91.35(8), O2–P1–Cl1 93.12(6), O2–P1–N2 87.13(8), O2–P1–N3 88.98(8), N1–P1–Cl1 94.19(7), N1–P1–N2 172.60(10), N1–P1–N3 91.74(9), Cl1–P1–N2 93.12(6), Cl1–P1–N3 173.65(7), N2–P1–N3 80.99(9).

We postulated that the instability of the dication **8** is, in part, due to the nucleophilicity of the chloride counterions, which compete for coordination with the DMAP ligands. For this reason we targeted an analogous dication, starting from the diiodide precursor, **4**, for which the halide is much softer. It was found that the iodide substituents are very readily displaced

10.1002/chem.201703119

from the phosphorus centre by dissolving samples in pyridine. By ^{31}P NMR spectroscopy, solutions obtained in this way exhibit a broad resonance at −103.5 ppm and a singlet at 168.3 ppm, corresponding to the parent geometry constrained compound **1**. Upon layering the mixture with hexane a red oil is formed, from which dark red crystals of $[P(ONO)(py)_3][I_3]_2$ ($[\mathbf{10}][I_3]_2$) can be grown after standing at room temperature. The identity of the counter ion again reflects the lability of the iodide substituents and also explains the observation of P(ONO) in the ^{31}P NMR spectrum, formed by reductive elimination of I_2. In solution there is no distinction between the coordinated pyridine and the pyridine solvent residue in the room temperature ^{1}H NMR spectrum and this is also the case at low temperature. The resonance in the ^{31}P NMR spectrum does, however, become significantly sharper upon cooling.

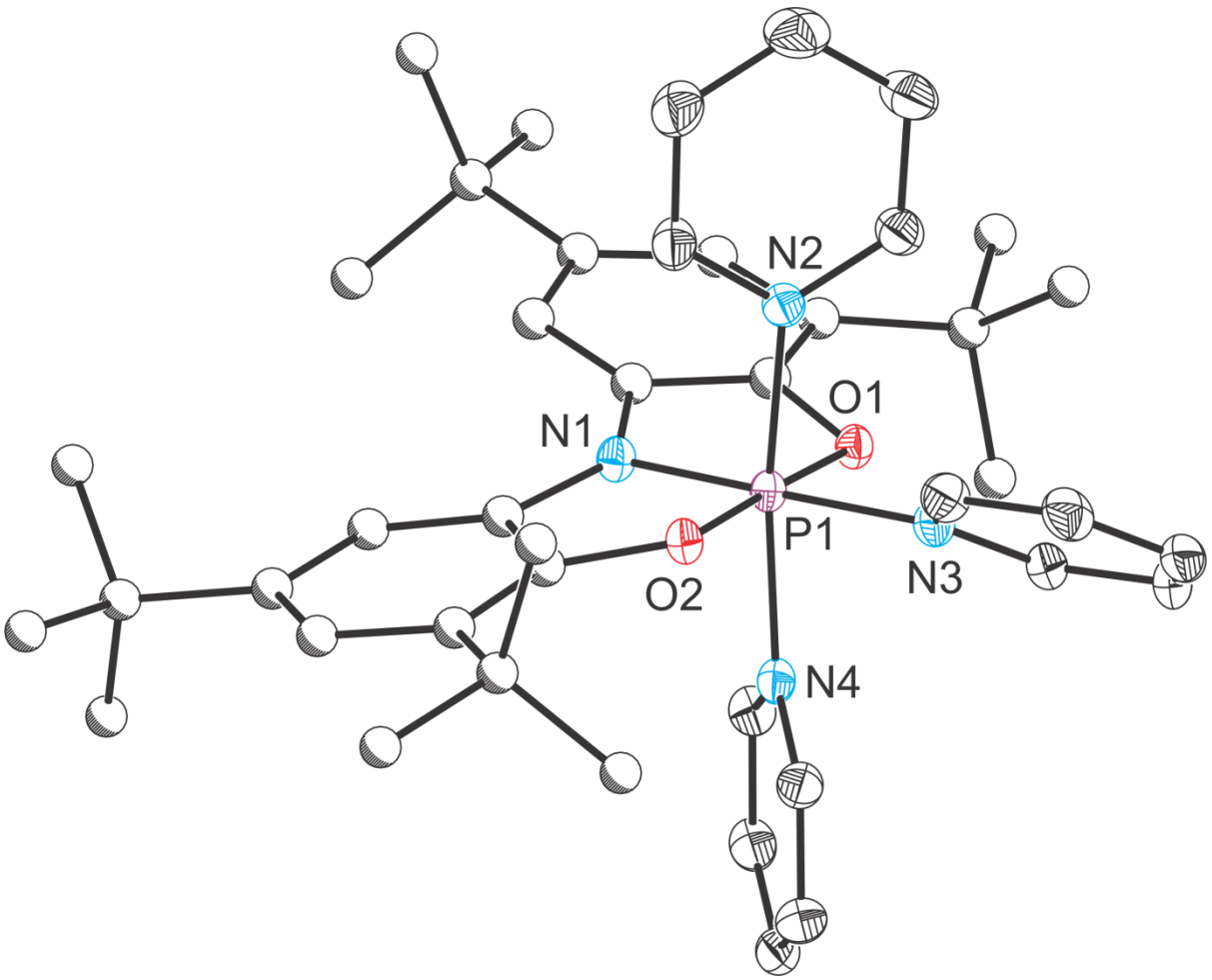

Figure 7. Structure of $[P(ONO)(py)_3]^{2+}$ (**10**). Thermal ellipsoids set at 50% probability; hydrogen atoms, solvent of crystallisation and triiodide counter anion are omitted for clarity. Selected bond lengths [Å] and angles [°]: P1–N1 1.704(3), P1–N2 1.939(3), P1–N3 1.873(3), P1–N4 1.931(3), P1–O1 1.662(2), P1–O2 1.654(2); O1–P1–O2 178.02(13), O1–P1–N1 90.29(13), O1–P1–N2 89.36(13), O1–P1–N3 89.07(13), O1–P1–N4 91.90(13), O2–P1–N1 90.78(13), O2–P1–N2 88.90(13), O2–P1–N3 89.88(13), O2–P1–N4 89.70(13), N1–P1–N2 94.11(14), N1–P1–N3 178.76(15), N1–P1–N4 92.98(14), N2–P1–N3 86.95(13), N2–P1–N4 172.79(13), N3–P1–N4 85.98(13).

The molecular structure of **10** (Figure 7) reveals a six-coordinate phosphorus centre in which the planar ONO^{3-} ligand assumes a meridional coordination mode and three pyridine molecules occupy the remaining octahedral coordination sites. Similar to the observations made for the monocationic compounds **7** and **9**, and the dicationic species **8**, the $P–N_{py}$ contact *trans* to the amide (1.873(3) Å) is longer than those orthogonal to this bond (1.939(3) and 1.931(3) Å). The P1–N1 bond of **10** (1.704(3) Å) is shorter than observed in both of the monocationic species, which is likely to be a consequence of both the weaker *trans* influence of the pyridine donor and the slightly greater positive charge on the phosphorus centre (calculated NBO charges at P for L(DMAP; **7**) = +2.221, L(bipy; **9**) = +2.207, L(py; **10**) = +2.426).

Having demonstrated the stepwise synthesis of phosphorus(V) cationic species utilising the phosphorus(III) precursor **2**, we were interested to see if analogous products could be formed via direct oxidation of **1** using standard chemical oxidising agents. The reaction of **1** with two equivalents of ferrocenium (as $[Fc]BAr^F_4$) in pyridine proceeds rapidly to give an orange solution that exhibits a single resonance in the ^{31}P NMR spectrum at −102.2 ppm, analogous

to that observed for **10** ($P(ONO)(py)_3$). Unfortunately crystallisation and isolation of analytically pure samples of this species has not been possible, although spectroscopic data evidences the formation of the product $[P(ONO)(py)_3][BAr^F{}_4]_2$. Interestingly, this reaction is not tolerant of common fluorinated anions, such as $[BF_4]^-$ and $[PF_6]^-$, resulting in decomposition arising from fluoride abstraction. Equally, the requirement to stabilise the dicationic phosphorus centre means that the oxidation only proceeds in pyridine.

Oxidation of **1** using oxygen gas (1 atm) proceeds slowly and requires heating benzene solutions to 70 °C over a period of several days. The ^{31}P NMR spectra of the reaction mixtures reveal consumption of **1** and the initial growth of two doublets at 119.4 and –46.7 ppm, related by a P–P coupling constant of 32 Hz. The ^1H NMR spectrum shows evidence for two independent ligand environments, one of which is desymmetrised, as observed by six resonances corresponding to the ^{t}Bu protons in a 1:1:1:1:2:2 ratio. The formation of this oxidation product (**11**) is accompanied by a colour change from colourless to dark purple, consistent with previously reported oxidation products of the ONO^{3-} ligand system.[17,26] The competing ligand decomposition appears to be unavoidable using O_2 and other oxygen-based oxidising agents such as trimethylamine *N*-oxide.

Upon continued heating of the reaction mixture **11** slowly converts to a second product **12**, also exhibiting two doublets in the ^{31}P NMR spectrum at –0.4 and –45.8 ppm with a reduced coupling constant of 25 Hz. The similar chemical shift of the upfield resonance compared to **11** suggests an analogous environment at this nucleus whereas the second is significantly upfield shifted and appears to be the site of the further reactivity. The ^1H NMR spectrum, however, is largely unchanged to that of **11**, suggesting a very subtle difference between the two products. By monitoring the oxidation of **1** by ^{31}P NMR spectroscopy, the reaction can

10.1002/chem.201703119

be halted at the appropriate time to allow isolation of either **11** or **12**, although neither can be completely separated from the purple ligand by products. However, crystals suitable for X-ray diffraction analysis could be grown for both species by cooling concentrated hexane solutions to −30°C and the molecular structures of each are presented in Figure 8.

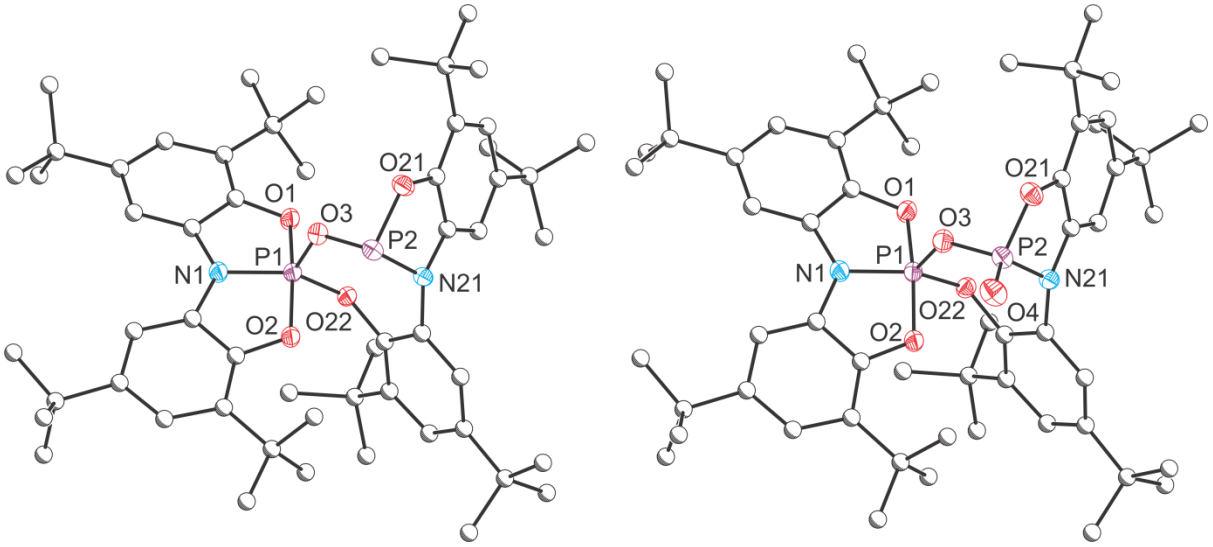

Figure 8. Molecular structure of [P(ONO)(μ^2-O)(μ^2:κ^1,κ^2-ONO)P] (**11**; left) and [P(ONO)(μ^2-O)(μ^2:κ^1,κ^2-ONO)P(O)] (**12**; right) (Thermal ellipsoids set at 50% probability; hydrogen atoms and solvent of crystallisation omitted for clarity). Selected bond lengths [Å] and angles [°]: **11**: P1–N1 1.702(2), P1–O1 1.662(2), P1–O2 1.691(2), P1–O3 1.592(2), P1–O22 1.633(2), P2–N21 1.700(2), P2–O21 1.634(2), P2–O3 1.672(2); O1–P1–O2 166.46(9), O1–P1–O3 96.52(9), O1–P1–O22 84.29(8), O1–P1–N1 88.60(8), O2–P1–O3 96.95(8), O2–P1–O22 90.08(8), O2–P1–N1 88.11(8), N1–P1–O3 110.08(9), N1–P1–O22 141.21(9), O3–P1–O22 108.61(8), P1–O3–P2 128.13(10), O21–P2–O3 97.36(8), O21–P2–N21 92.10(9), O3–P2–N21 101.13(8). **12**: P1–N1 1.698(2), P1–O1 1.659(2), P1–O2 1.677(2), P1–O3 1.619(2), P1–O22 1.633(2), P2–N21 1.664(2), P2–O21 1.604(2), P2–O3 1.604(2) P2–O4 1.445(2); O1–P1–O2 166.27(10), O1–P1–O3 96.44(9), O1–P1–O22 84.24(9), O1–P1–N1 88.75(9), O2–P1–O3 97.22(9), O2–P1–O22 90.48(9), O2–P1–N1 88.43(9), N1–P1–O3 107.75(9), N1–P1–O22 145.36(10), O3–P1–O22 106.73(9), P1–O3–P2 129.60(11), O21–P2–

O3 101.53(9), O21–P2–N21 95.18(10), O21–P2–O4 117.02(11), O3–P2–N21 105.95(10), O3–P2–O4 113.90(11), N1–P2–O4 120.27(11).

The molecular structure of **11** reveals a phosphorus(III)/phosphorus(V) mixed valence species in which the two phosphorus centres are connected by a bridging oxide (∠P1–O3–P2 = 128.13(10)°). The phosphorus(V) centre is also coordinated by a phenoxide arm, which has been displaced from P2. P1 exhibits a distorted square-base pyramidal geometry (τ = 0.42) and P2 a pyramidal geometry (Σ_{angles}(P2) = 291°). The ONO^{3-} ligand assumes a planar conformation about P1 with the bonds to phosphorus similar in length to those observed in related phosphorus(V) compounds. The bridging oxide (O3) occupies the pseudo axial position at P1, exhibiting the shortest of the P1–O bonds (1.592(2) Å) whilst the P1–O22 bond is also slightly shortened relative to those within the tridentate ligand system (1.633(2) Å). The P2–O3 bond is significantly longer than the analogous bond to P1 due to the lower valency of the phosphorus centre, however, P2–O21 is slightly shorter than the related bonds to P1, which is possibly due to the lower geometric constraint around P2. The P2–N21 bond is the same within error to that of P1–N1.

In the solid state **12** is near isostructural to **11** with exception of the formation of a phosphine oxide at P2. Whilst the bond metrics around P1 are very similar to those observed in **11**, the bonds about P2 are all significantly contracted due to the increased valency of the phosphorus centre. This is also accompanied by an increase in the bond angles around P2 relative to those in **11**. The P=O bond (1.445(2) Å) is typical for heteroatom-substituted phosphine oxides.

10.1002/chem.201703119

*2.3. Reduction of **1***

The one electron reduction of **1** using a stoichiometric amount of KC_8 at room temperature immediately delivers a bright yellow solution containing a single NMR active product $[K]_2[\mathbf{13}]$, which is extremely air-sensitive, with solutions rapidly turning colourless upon exposure to air. The ^{31}P NMR spectrum exhibits a singlet resonance at 94.1 ppm, which is significantly upfield shifted from that observed for **1** (169.4 ppm). The ^{1}H NMR spectrum reveals four resonances corresponding to the aromatic backbone of the ligand and four resonances corresponding to the ^{t}Bu protons, which highlights an unsymmetrical ligand geometry in solution. It is also apparent that a two electron reduction to form the dianion of **1** is not possible using multiple equivalents of KC_8, with only the formation of **13** observed in such experiments.

Using 2,2,2-crypt as a cation sequestering agent, crystals suitable for X-ray diffraction analysis were grown by slow diffusion of hexane into a concentrated THF solution and the molecular structure is pictured in Figure 9. It is noteworthy that the NMR spectra data for $[K(2,2,2\text{-crypt})]_2[\mathbf{13}]$ is analogous to that obtained without the cation sequestering agent.

10.1002/chem.201703119

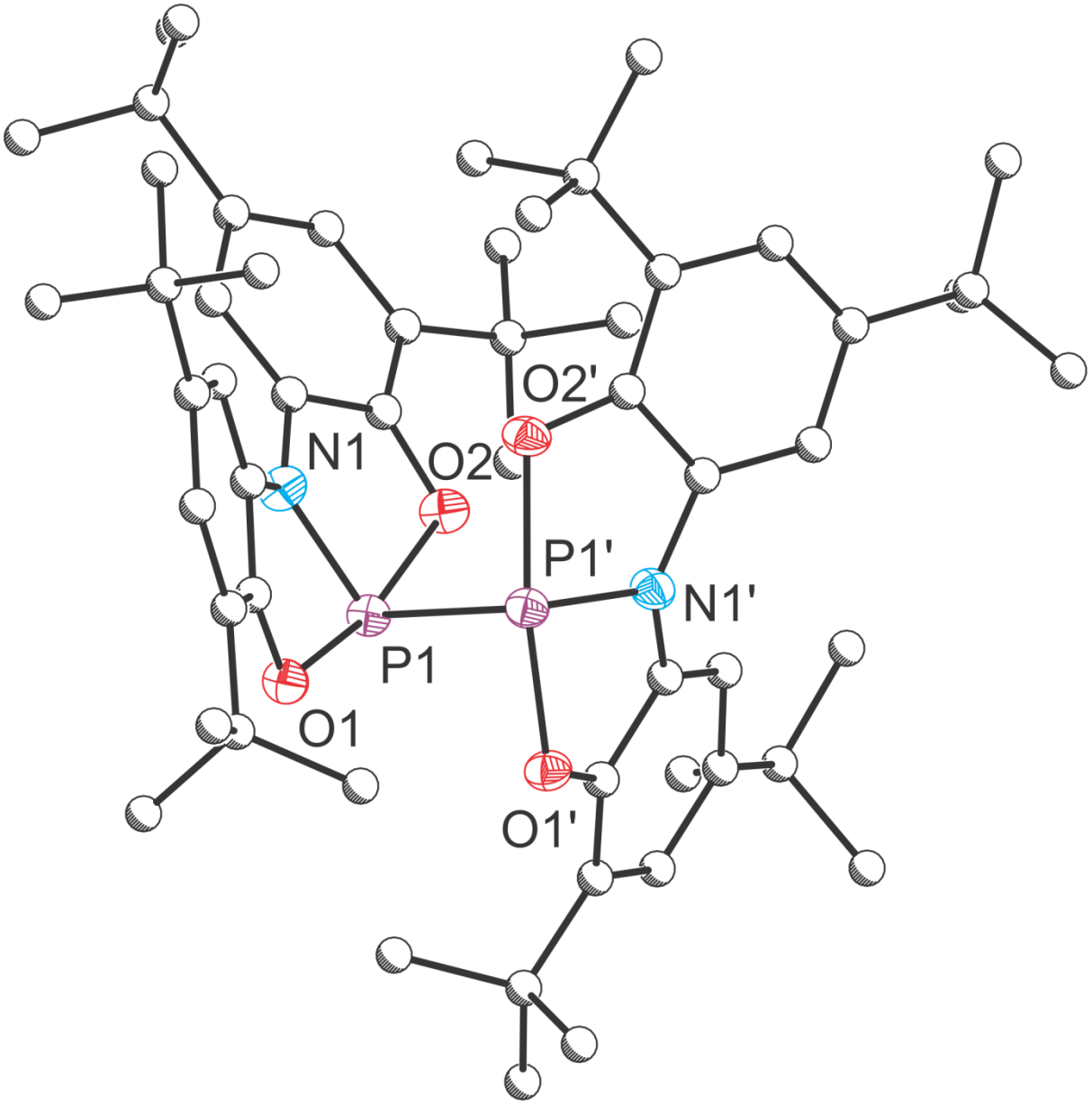

Figure 9. Structure of $[\{P(ONO)\}_2]^{2-}$ (**13**). Thermal ellipsoids set at 50% probability; hydrogen atoms and $[K(2,2,2\text{-crypt})]^+$ omitted for clarity. Selected bond lengths [Å] and angles [°]: P1–P1′ 2.287(1), P1–N1 1.768(1), P1–O1 1.897(1), P1–O2 1.932(1); O1–P1–O2 165.58(3), O1–P1–N1 82.95(3), O1–P1–P1′ 85.07(2), O2–P1–N1 83.86(4), O2–P1–P1′ 92.72(2), N1–P1–P1′ 105.00(3). Symmetry operation ′: 1–x, y, 1.5–z.

The molecular structure of **13** reveals two $P(ONO)^-$ moieties, bridged by a P–P bond (2.2868(5) Å) with both ligands adopting planar conformations. The N1–P1–P1′–N1′ torsion

angle of 115.43° shows a significant twist between each half of the dimer, reducing steric repulsions. The P–P bond length lies well within the range expected for a two electron single bond. The potassium counter ions are well sequestered and do not interact with **13**. The P–O bond lengths (1.897(1) and 1.932(1) Å) are unsymmetrical and significantly lengthened relative to those of **1**, whereas the P–N bond is very similar to that of the parent complex. This is in analogy to the structures of the *tert*-butoxide and diphenylamide adducts of **1** that have recently been reported.[8] Coupled with the ^{1}H NMR data recorded for **13** the long P−O bonds suggest lability of one of the phenoxide arms in solution.

The formation of **13** suggests that the reaction with KC_8 forms a highly unstable P-centred radical that rapidly combines with a second radical anion to form the dianionic P–P bonded dimer. The instability of such a radical was probed through the reaction of **1** with a single equivalent of the stable radical TEMPO. Reaction mixtures in C_6D_6 revealed a 1:1 ratio of unreacted **1** and a new product (**14**) exhibiting a singlet in the ^{31}P NMR spectrum at −29.9 ppm. Addition of a second equivalent of TEMPO results in full consumption of **1**. Crystals of **14** were grown by cooling a concentrated hexane solution to −30 °C. The molecular structure (Figure 10) reveals a five-coordinate phosphorus centre coordinated by a planar ONO ligand and two TEMPO moieties in trigonal bipyramidal geometry (τ = 0.88). The equatorial P–O_{TEMPO} bonds are slightly shorter than those of the axial P–O bonds to the ligand and the TEMPO N–O bonds are significantly elongated relative to free TEMPO (1.284(8) Å) due to its reduction to the anionic form.[27]

10.1002/chem.201703119

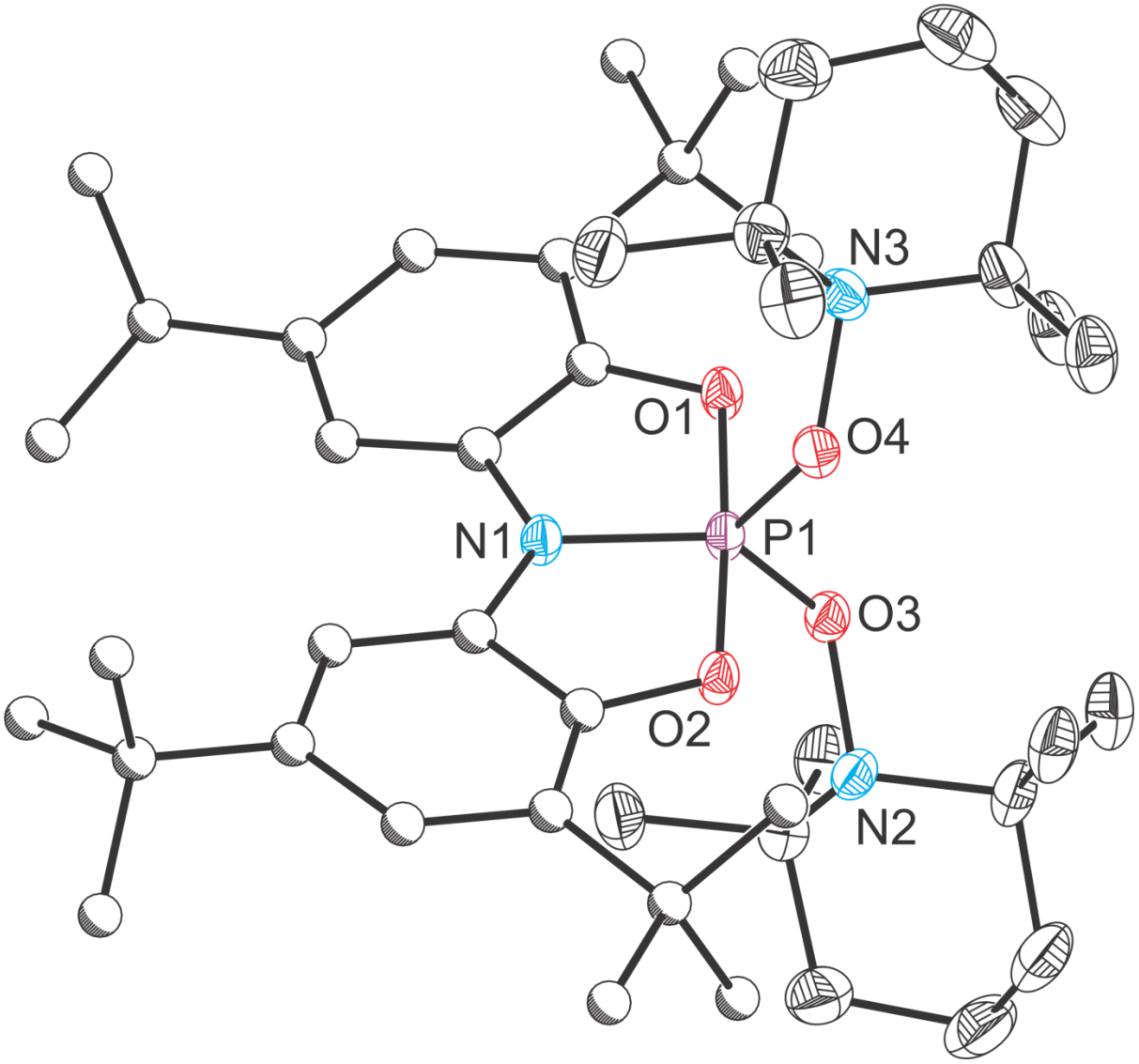

Figure 10. Molecular structure of P(ONO)(TEMPO)$_2$ (**14**). Thermal ellipsoids set at 50% probability; hydrogen atoms and solvent of crystallisation are omitted for clarity. Selected bond lengths [Å] and angles [°]: P1–N1 1.697(1), P1–O1 1.684(1), P1–O2 1.685(1), P1–O3 1.619(1), P1–O4 1.622(1), N2–O3 1.473(1), N3–O4 1.473(1); O1–P1–O2 176.82(4), O1–P1–O3 87.06(4), O1–P1–O4 94.72(4), N1–P1–O1 88.47(4), N1–P1–O2 88.38(4), N1–P1–O3 122.96(5), N1–P1–O4 123.95(5), O2–P1–O3 95.02(4), O2–P1–O4 86.69(4), O3–P1–O4 113.09(5).

3. Conclusions

We have thoroughly explored the reactivity of a geometrically constrained phosphorus(III) complex supported by the *N*,*N*-bis(3,5-di-tert-butyl-2-phenolate)amide pincer ligand (P(ONO); **1**) towards a range of molecular oxidants and reductants in order to establish whether redox processes play a role in the ability of **1** to activate small molecule substrates (such as ammonia and water). These studies show that **1** can be readily oxidized to afford a series of novel phosphorus(V) compounds including rare species such as a phosphorus(V) diiodide, $P(ONO)I_2$ (**4**). The lability of the halide ions substituents of the dichloride compound, $P(ONO)Cl_2$ (**2**), towards a number of strong Lewis bases was also explored, demonstrating the one chloride ion can be readily displaced to generate monocationic species such as, $[P(ONO)Cl(DMAP)_2]^+$ (**7**), whereas the generation of dicationic compounds is less straightforward, often giving rise to mixtures of compounds that are in equilibria. The chemical reduction of **1** was also explored affording a species with a direct P–P bond. Attempts to generate a radical species from the reaction of **1** with TEMPO resulted in the clean formation of $P(ONO)(TEMPO)_2$ (**14**). It is worth noting that in all of the redox transformations, changes in oxidation state occur at the phosphorus element centre and that the *N*,*N*-bis(3,5-di-tert-butyl-2-phenolate)amide ligand does not seem to be involved to any significant extent.

4. Experimental

Solvents and Reagents. Hexane (hex; Sigma-Aldrich, ≥97.0%), CH_2Cl_2 (HPLC grade, ≥99.8%, Sigma-Aldrich) and toluene (Sigma-Aldrich, 99.9%) were dried using an MBraun SPS-800 solvent system. Tetrahydrofuran (THF; Sigma-Aldrich, ≥99.9%) was dried over a potassium metal/benzophenone mixture. Pyridine (py; Alfa Aesar, 99+%) and $CHCl_3$ (Honeywell, ≥99.8%) were distilled from CaH_2 and stored over 3 Å molecular sieves. C_6D_6

(Aldrich, 99.6%) and d_5-pyridine (Cambridge Isotope Laboratories Inc., 99.5%) were dried over 3 Å molecular sieves. CD_2Cl_2 (Euriso-top, 99.90%), d_8-THF (Euriso-top, 99.50%) and d_8-toluene (Sigma Aldrich, 99.6%) were dried over CaH_2 and stored over activated 3 Å molecular sieves. P(ONO) and [Fc][BAr_4^F] were synthesized according to previously reported synthetic procedures.[6,28] KC_8 was prepared by heating a stoichiometric mixture of graphite powder and potassium to 250 °C for several days under argon. PCl_5 (Acros Organics, 98%), PBr_5 (Fisher Scientific, 95%), I_2 (Fisher Scientific, Analytical grade), XeF_2 (VWR, 99.5+%), KF (Sigma Aldrich, 99%), DMAP (Sigma Aldrich, ReagentPlus®, ≥99%), O_2 (BOC), TEMPO (Alfa Aesar, 98+%), 4,7,13,16,21,24-hexaoxa-1,10-diazabicyclo[8,8,8]-hexacosane (2,2,2-crypt; VWR, 99%) were used as received.

*Synthesis of P(ONO)Cl₂ (**2**).* Compound **1** (200 mg, 0.441 mmol) and PCl_5 (92 mg, 0.441 mmol) were dissolved in toluene (5 mL). The solution was stirred at room temperature for 12 hours after which all volatiles were removed *in vacuo*. The residue was extracted into toluene and filtered via cannula. The resulting solution was concentrated until precipitation occurred and the solid was then dissolved with gentle heating. Colourless crystals of $P(ONO)Cl_2$ were then grown at −30 °C and isolated by filtration. Yield: 156 mg (67%). Anal. Calcd for $C_{28}H_{40}Cl_2NO_2P$ (524.19 g mol^{-1}): C 64.12, H 7.69, N 2.67; Found: C 64.42, H 7.62, N 2.74. ^{1}H NMR (C_6D_6, 298 K, 400.20 MHz): δ (ppm) 7.58–7.57 (m, 2H; CH), 7.19–7.17 (m, 2H; CH), 1.52 (s, 18H; ^{t}Bu), 1.34 (s, 18H; ^{t}Bu). ^{1}H{^{31}P} NMR (C_6D_6, 298 K, 400.20 MHz): δ (ppm) 7.58 (d, $^4J_{H–H}$ = 2 Hz; CH), 7.18 (d, $^4J_{H–H}$ = 2 Hz; CH) all other resonances as above. ^{31}P NMR (C_6D_6, 298 K, 162.00 MHz): δ (ppm) −21.0. ^{13}C{^{1}H} NMR (C_6D_6, 298 K, 100.63 MHz): δ (ppm) 145.1 (s, Ar-C), 141.1 (d, $J_{C–P}$ = 6 Hz; Ar-C), 134.0 (d, $J_{C–P}$ = 10 Hz; Ar-C), 126.7 (d, $J_{C–P}$ = 27 Hz; Ar-C), 117.0 (s; Ar-CH), 106.9 (d, $J_{C–P}$ = 16 Hz; Ar-CH), 35.1 (s; ^{t}Bu-C), 34.7 (s; ^{t}Bu-C), 31.8 (s; ^{t}Bu-CH_3), 29.7 (s; ^{t}Bu-CH_3).

*Synthesis of P(ONO)Br$_2$ (**3**).* Compound **1** (100 mg, 0.220 mmol) and PBr_5 (94.9 mg, 0.220 mmol) were dissolved in toluene (5 mL). The yellow solution was stirred for thirty minutes after which all volatiles were removed *in vacuo*. The residue was extracted into toluene and filtered away from an insoluble white precipitate. Yellow plate crystals were grown from a concentrated toluene solution at −30 °C. Yield: 52.7 (39%). Anal. Calcd for $C_{28}H_{40}Br_2NO_2P$ (613.09 g mol^{-1}): C 54.83, H 6.57, N 2.28; Found: C 55.03, H 6.61, N 2.25. ^{1}H NMR (C_6D_6, 298 K, 400.20 MHz): δ (ppm) 7.61–7.58 (m, 2H; CH), 7.20–7.18 (m, 2H; CH), 1.55 (s, 18H; ^{t}Bu), 1.34 (s, 18H; ^{t}Bu). ^{1}H{^{31}P} NMR (C_6D_6, 298 K, 400.20 MHz): δ (ppm) 7.60 (d, $^4J_{H–H}$ = 2 Hz; CH), 7.19 (d, $^4J_{H–H}$ = 2 Hz; CH) all other resonances as above. ^{31}P NMR (C_6D_6, 298 K, 161.99 MHz): δ (ppm) −88.2 (s). ^{13}C{^{1}H} NMR (C_6D_6, 298 K, 100.63 MHz): δ (ppm) 145.2 (s; Ar-C), 142.0 (d, $J_{C–P}$ = 10 Hz; Ar-C), 134.0 (d, $J_{C–P}$ = 9 Hz; Ar-C), 126.4 (d, $J_{C–P}$ = 27 Hz; Ar-C), 117.2 (s, Ar-CH), 107.0 (d, $J_{C–P}$ = 6 Hz; Ar-CH), 35.1 (s; ^{t}Bu-C), 34.7 (s; ^{t}Bu-C), 31.7 (s; ^{t}Bu-CH_3), 29.8 (s; ^{t}Bu-CH_3).

*Synthesis of P(ONO)I$_2$ (**4**).* Compound **1** (150 mg, 0.331 mmol) and I_2 (84 mg, 0.331 mmol) were dissolved in toluene (3 mL) to give a dark red solution. The solution was stirred for one hour after which all volatiles were removed *in vacuo*, leaving an orange solid. The solid was extracted into toluene and concentrated until an orange precipitate formed. This was gently warmed back into solution, which was then cooled to −30 °C, yielding large orange block-shaped crystals. The crystals were isolated by filtration. Yield: 154 mg (66%). Anal. Calcd for $C_{28}H_{40}Br_2NO_2P$ (707.09 g mol^{-1}): C 47.54, H 5.70, N 1.98; Found: C 47.88, H 5.79, N 1.99. ^{1}H NMR (C_6D_6, 298 K, 499.93 MHz): δ (ppm) 7.63 (d, $^4J_{H–H}$ = 2 Hz, 2H; CH), 7.18 (d, $^4J_{H–H}$ = 2 Hz, 2H; CH), 1.56 (s, 18H; ^{t}Bu), 1.32 (s, 18H; ^{t}Bu). ^{31}P NMR (C_6D_6, 298 K, 202.38 MHz): δ (ppm) −258.3. ^{13}C{^{1}H} NMR (C_6D_6, 298 K, 125.71 MHz): δ (ppm) 143.3 (s; Ar-C), 141.0 (d, $J_{C–P}$ = 13Hz; Ar-C), 131.5 (d, $J_{C–P}$ = 5 Hz; Ar-C), 124.1 (d, $J_{C–P}$ = 26 Hz; Ar-C),

115.3 (s; Ar-CH), 105.2 (d, $J_{C–P}$ = 15 Hz; Ar-CH), 33.1 (s; ^{t}Bu-C), 32.7 (s; ^{t}Bu-C), 29.7 (s; ^{t}Bu-CH_3), 28.1 (s; ^{t}Bu-CH_3).

*Synthesis of P(ONO)(H)F (**5**).* Compound **1** (100 mg, 0.220 mmol) was dissolved in toluene (2 mL) and the solution was cooled to −30 °C. XeF_2 (37 mg, 0.22 mmol) was added to the stirred solution gradually resulting in the colourless solution turning yellow then dark red. After stirring the solution at room temperature for one hour, all volatiles were removed *in vacuo*. The red residue was extracted into hot hexane and filtered via cannula. The solution was concentrated and cooled to −30 °C, yielding red crystals that were isolated by filtration. Crude yield: 67 mg (64%); product contains a small amount of $P(ONO)F_2$ impurity. ^{1}H NMR (C_6D_6, 298 K, 400.20 MHz): δ (ppm) 7.91 (dd, $^{1}J_{H–P}$ = 948 Hz, $^{2}J_{H–F}$ =89 Hz, 1H; PH), 7.77 (s, 2H; CH), 7.23 (s, 2H; CH), 1.54 (s, 18H; ^{t}Bu), 1.41 (s, 18H; ^{t}Bu). ^{1}H{^{31}P} NMR (C_6D_6, 298 K, 499.93 MHz): δ (ppm) 7.91 (d, $^{2}J_{H–F}$ = 89 Hz, 1H; P*H*), all other resonances the same as above. ^{31}P NMR (C_6D_6, 298 K, 162.00 MHz): δ (ppm) −31.9 (dd, $^{1}J_{P–H}$ = 948 Hz, $^{1}J_{P–F}$ = 1048 Hz). ^{31}P{^{1}H} NMR (C_6D_6, 298 K, 162.00 MHz): δ (ppm) −31.9 (d, $^{1}J_{P–F}$ = 1048 Hz). ^{19}F NMR (C_6D_6, 298 K, 376.56 MHz): δ (ppm) −61.7 (dd, $^{1}J_{F–P}$ = 1048 Hz, $^{2}J_{F–H}$ = 89 Hz). ^{19}F{^{1}H} NMR (C_6D_6, 298 K, 376.56 MHz): δ (ppm) −61.7 (d, $^{1}J_{F–P}$ = 1048 Hz). ^{13}C{^{1}H} NMR (C_6D_6, 298 K, 100.63 MHz): δ (ppm) 143.9 (Ar-C), 141.0 (dd, $J_{C–P}$ = 7 Hz, $J_{C–F}$ = 2 Hz; Ar-C), 133.6 (d, $J_{C–P}$ = 6 Hz; Ar-C), 128.1 (Ar-C, resonance hidden beneath solvent residue peak, located through HMBC measurements), 116.4 (Ar-CH), 106.9 (d, $J_{C–P}$ = 16 Hz; Ar-CH), 35.1 (^{t}Bu-C), 34.8 (^{t}Bu-C), 31.9 (^{t}Bu-CH_3), 29.8 (s; ^{t}Bu-CH_3).

*Synthesis of $P(ONO)F_2$ (**6**).* Compound **1** (150 mg, 0.286 mmol) and KF (160 mg, 2.85 mmol) were added to an ampoule fitted with a gas tight valve, and toluene (2 mL) was added. The mixture was stirred at 80 °C for five days, after which the solution was filtered via

cannula. All volatiles were removed *in vacuo* to give a colourless solid, which was extracted into hexane. The solution was concentrated and cooled to −30 °C to give colourless crystals. Yield: 15 mg (11%). Anal. Calcd: C 68.41, H 8.20, N 2.85. Found: C 69.42, H 8.45, N 2.89. ^{1}H NMR (C_6D_6, 298 K, 400.17 MHz): δ (ppm) 7.57–7.55 (m, 2H; CH), 7.20–7.18 (d, 2H; CH), 1.51 (s, 18H; ^{t}Bu), 1.38 (s, 18H; ^{t}Bu). ^{1}H{^{31}P} NMR (C_6D_6, 298 K, 400.20 MHz) 7.56 (d, $^{4}J_{H–H}$ = 2 Hz; CH), 7.19 (d, $^{4}J_{H–H}$ = 2 Hz; CH), all other resonances as above. ^{31}P NMR (C_6D_6, 298 K, 161.99 MHz): δ (ppm) −38.2 (t, $^{1}J_{P–F}$ = 879 Hz). ^{31}P{^{1}H} NMR (C_6D_6, 298 K, 161.99 MHz): δ (ppm) −38.2 (t, $^{1}J_{P–F}$ = 879 Hz). ^{19}F NMR (C_6D_6, 298 K, 376.54 MHz): δ (ppm) −55.7 (d, $^{1}J_{F–P}$ = 879 Hz). ^{19}F{^{1}H} NMR (C_6D_6, 298 K, 376.54 MHz): δ (ppm) −55.7 (d, $^{1}J_{F–P}$ = 879Hz). ^{13}C{^{1}H} NMR (C_6D_6, 298 K, 125.71 MHz) δ (ppm) 145.1 (Ar-C), 138.6 (dt, $J_{C–P}$ = 4 Hz, $J_{C–F}$ = 2 Hz; Ar-C), 134.1 (dt, $J_{C–P}$ = 13 Hz, $J_{C–F}$ = 1 Hz; Ar-C), 128.1 (Ar-C, resonance hidden beneath residue solvent resonance, located using HMBC experiment), 116.7 (Ar-CH), 106.6 (d, $J_{C–P}$ = 15.7 Hz; Ar-CH), 35.1 (^{t}Bu-C), 34.7 (^{t}Bu-C), 31.8 (^{t}Bu-CH_3), 29.8 (^{t}Bu-CH_3).

Synthesis of [P(ONO)(Cl)(DMAP)$_2$]Cl ([7]Cl). Compound **2** (100 mg, 0.220 mmol) was dissolved in dichloromethane (1 mL) and to the solution was added DMAP (53.9 mg, 0.440 mmol). The pale yellow solution was stirred for 15 minutes and then filtered into an ampoule. Colourless crystals of the product were grown by layering the solution with hexane and were isolated by filtration. Yield: 65 mg (42%). A satisfactory elemental analysis could not be obtained for this compound. ^{1}H NMR (CD_2Cl_2, 298 K, 400.17 MHz): δ (ppm) 8.08 (br, 4H; DMAP-CH), 7.35 (s, 2H; ONO-CH), 7.03 (s, 2H, ONO-CH), 6.68 (br, 4H; DMAP-CH), 3.23 (br, 12H; DMAP-CH_3), 1.44 (s, 18H; ^{t}Bu), 1.38 (s, 18H; ^{t}Bu). ^{1}H NMR (CD_2Cl_2, 223 K, 400.20 MHz): 8.63–8.59 (m, 2H; DMAP-CH), 7.66–7.62 (m, 2H; DMAP-CH), 7.31 (s, 2H; ONO-CH), 6.98 (s, 2H; ONO-CH), 6.76 (d, $^{3}J_{H–H}$ = 6 Hz, 2H; DMAP-CH), 6.49 (d, $^{3}J_{H–H}$ =

6.9 Hz, 2H; DMAP-CH), 3.31 (s, 6H; DMAP-CH_3), 3.12 (s, 6H; DMAP-CH_3), 1.38 (s, 18H; *t*Bu), 1.33 (s, 18H; *t*Bu). $^{31}P\{^1H\}$ NMR (CD_2Cl_2, 223 K, 161.99 MHz) δ (ppm) –101.7 (br s). $^{31}P\{^1H\}$ NMR (CD_2Cl_2, 223 K, 161.99 MHz) δ (ppm) –101.7 (s). $^{13}C\{^1H\}$ NMR (CD_2Cl_2, 298 K, 100.63 MHz): δ (ppm) 156.8 (DMAP-C), 145.8 (ONO-C), 142.8 (br; DMAP-C), 139.2 (ONO-C), 134.4 (d, $J_{C–P}$ = 11 Hz; ONO-C), 130.3 (d, $^2J_{C–P}$ = 19 Hz; DMAP-CH), 116.4 (ONO-CH), 106.8 (d, $J_{C–P}$ = 17 Hz; ONO-CH), 106.6 (br; DMAP-CH), 40.6 (DMAP-CH_3), 35.3 (^{t}Bu-C), 34.6 (^{t}Bu-C), 31.8 (^{t}Bu-CH_3), 30.2 (^{t}Bu-CH_3).

*Synthesis of [P(ONO)(DMAP)$_3$]Cl$_2$ ([**8**]Cl).* **2** (100 mg, 0.191 mmol) and DMAP (93.2 mg, 0.763 mmol) were added to an ampoule and dissolved in $CHCl_3$ (1 mL) to give a pale yellow solution. When left to stand colourless crystals of $[P(ONO)(DMAP)_3][Cl]_2 \cdot 7CHCl_3$ formed, which were isolated by decanting away the mother liquor and drying *in vacuo*. Yield: 102 mg (45%; yield includes solvent observed in elemental analysis). Anal. Calcd for $C_{49}H_{70}Cl_2N_7O_2P_1 \cdot 2.6(CHCl_3)$: C 52.86, H 6.25, N 8.41. Found: C 52.83, H 6.53, N 8.51. ^1H NMR (CD_2Cl_2, 223 K, 499.93 MHz): δ (ppm) 8.01–7.98 (m, 2H; DMAP-CH), 7.51 (br s, 4H; DMAP-CH), 7.14 (s, 2H; ONO-CH), 7.00–6.96 (m, 2H; DMAP-CH) 6.86 (s, 2H; ONO-CH), 3.41 (s, 6H; DMAP-CH_3), 3.10 (s, 12H; DMAP-CH_3), 1.36 (s, 18H; ^{t}Bu), 1.25 (s, 18H; ^{t}Bu). ^{31}P NMR ($CDCl_3$, 298 K, 162.00 MHz): δ (ppm) −117.3 (v br). $^{31}P\{^1H\}$ NMR (CD_2Cl_2, 223 K, 202.38 MHz): δ (ppm) −118.4 (s). $^{13}C\{^1H\}$ NMR (CD_2Cl_2, 223 K, 125.71 MHz): δ (ppm) 155.0 (DMAP-C), 155.6 (DMAP-C), 145.8 (ONO-C), 141.5 (DMAP-CH), 140.3 (br; DMAP-CH), 138.7 (ONO-C), 133.5 (d, $J_{C–P}$ = 10 Hz; ONO-C), 128.4 (d, $J_{C–P}$ = 24 Hz; ONO-C), 116.0 (ONO-CH), 107.7 (d, $J_{C–P}$ = 8 Hz; DMAP-CH), 106.4 (br; DMAP-CH), 105.3 (d, $J_{C–P}$ = 14 Hz; ONO-CH), 41.1 (DMAP-CH_3), 40.3 (DMAP-CH_3), 34.7 (^{t}Bu-C), 34.1 (^{t}Bu-C), 31.0 (^{t}Bu-CH_3), 29.7 (^{t}Bu-CH_3). ESI-MS (+ve mode, CH_2Cl_2) Calculated for $C_{42}H_{61}N_5O_3P_1 \cdot H_2O$ (P(ONO)(DMAP)$_2$(OH)·H_2O) = 732.4618; Observed *m*/*z* = 732.6375.

*Synthesis of [P(ONO)(Cl)(bipy)][BAr$^{F}_{4}$] ([**9**][BAr$^{F}_{4}$]).* A Schlenk tube was charged with **2** (50 mg, 0.095 mmol), 2,2′-bipyridine (15mg, 0.095 mmol) and Na[BAr$^{F}_{4}$] (84 mg, 0.095 mmol) and $CHCl_3$ (2 mL) was added. The mixture was sonicated for 20 minutes with the solution going from pale yellow to dark green. After stirring at room temperature for 12 hours the solution was filtered into an ampoule and layered with hexane, resulting in the formation of brown/gold crystals of [**7**]Cl·4.5CH_2Cl_2·hex. The crystals were isolated by filtration and mechanically separated from a small amount of unreacted Na[BAr$^{F}_{4}$]. Yield: 76 mg (53%). Anal. Calcd for $C_{70}H_{60}BClF_{24}N_3O_2P$ (1507.86 g mol^{-1}): C 55.74, H 4.01, N 2.79; Found: C 55.96, H 3.98, N 2.85. ^{1}H NMR (CD_2Cl_2, 298 K, 400.20 MHz): δ (ppm) 10.77 (dd, $^{3}J_{H–P}$ = 12 Hz, $^{3}J_{H–H}$ = 6 Hz, 1H; bipy-CH), 8.77–8.73 (m, 1H; bipy-CH), 8.68–8.65 (m, 1H; bipy-CH), 8.64–8.60 (m, 1H; bipy-CH), 8.50–8.46 (m, 1H; bipy-CH), 8.42–8.37 (m, 1H; bipy-CH), 8.34–8.28 (m, 1H; bipy-CH), 7.91–7.85 (m, 1H; bipy-CH), 7.76–7.72 (m, 8H; [BAr$^{F}_{4}$]$^{–}$), 7.55 (s, 4H; [BAr$^{F}_{4}$]$^{–}$), 7.54–7.53 (m, 2H; ONO-CH), 7.04–7.02 (m, 2H; ONO-CH), 1.42 (s, 18H; ^{t}Bu), 1.06 (s, 18H; ^{t}Bu). ^{31}P NMR (CD_2Cl_2, 298 K, 162.00 MHz) δ (ppm) −77.2. ^{11}B NMR (CD_2Cl_2, 298 K, 128.39 MHz) δ (ppm) −6.59. ^{19}F NMR (CD_2Cl_2, 298 K, 376.54 MHz) δ (ppm) −62.8. ^{13}C{^{1}H} NMR (CD_2Cl_2, 298 K, 100.63 MHz) δ (ppm) 162.2 (q, $^{1}J_{C–B}{}^{11}$ = 50 Hz; BAr$^{F}_{4}$-C), 148.3 (bipy-CH), 147.2 (ONO-C), 146.9 (d, $J_{C–P}$ = 6 Hz; bipy-C), 145.5 (bipy-CH), 143.9 (bipy-CH), 140.8 (bipy-C), 138.8 (ONO-Ar-C), 135.8 (d, $J_{C–P}$ = 8 Hz; bipy-CH), 135.5 (d, $J_{C–P}$ = 12 Hz; ONO-C), 135.2 (BAr$^{F}_{4}$-CH), 131.0 (d, $J_{C–P}$ = 3 Hz; bipy-CH), 130.3 (d, $J_{C–P}$ = 7 Hz; bipy-CH), 129.3 (qq, $J_{C–F}$ = 32 Hz, $J_{C–F}$ = 3 Hz; BAr$^{F}_{4}$-C(CF_3)), 128.8 (ONO-C), 125.1 (q, $^{1}J_{C–F}$ = 273 Hz; BAr$^{F}_{4}$-CF_3), 123.3 (d, $J_{C–P}$ = 5 Hz; bipy-CH), 123.2 (d, $J_{C–P}$ = 4 Hz; bipy-CH), 117.9 (sept, $J_{C–P}$ = 4 Hz; BAr$^{F}_{4}$-CH), 117.7 (ONO-CH), 107.1 (d, $J_{C–P}$ = 16 Hz, ONO-CH), 35.4 (^{t}Bu-C), 34.6 (^{t}Bu-C), 31.7 (^{t}Bu-CH_3), 29.4 (^{t}Bu-CH_3). ESI-MS (+ve mode, CH_2Cl_2): Calcd for $C_{38}H_{48}ClN_3O_2P$: 644.3173 Da; Observed *m*/*z* 644.5138.

*Synthesis of [P(ONO)(py)$_3$][I$_3$]$_2$ ([**10**][I$_3$]$_2$).* Compound **4** (100 mg, 0.141 mmol) was dissolved in pyridine (0.5 mL) and the solution was layered with hexane. Upon standing at room temperature a red oil formed which crystallised to give large red blocks over a period of two weeks. Yield: 40 mg (58 %). ^{1}H NMR (d_5-pyridine, 298 K, 400.17 MHz): δ (ppm) 7.75–7.73 (m, 2H; CH), 7.32–7.30 (m, 2H; CH), 1.71 (s, 18H; ^{t}Bu), 1.32 (s, 18H; ^{t}Bu). ^{31}P NMR (d_5-pyridine, 298 K, 161.99 MHz) δ (ppm) −102.8 (br s). ^{13}C{^{1}H} NMR (d_5-pyridine, 298 K, 125.71 MHz): δ (ppm) 149.0 (Ar-C), 139.8 (Ar-C), 136.2 (Ar-C, resonance hidden beneath residue solvent resonance, located using HMBC experiment), 129.1 (d, $J_{C–P}$ = 24 Hz; Ar-C), 119.2 (Ar-CH), 107.5 (d, $^3J_{C–P}$ = 14 Hz; Ar-CH), 35.7 (^{t}Bu-C), 35.6 (^{t}Bu-C), 31.8 (^{t}Bu-CH$_3$), 31.6 (^{t}Bu-CH$_3$).

*Oxidation of **1** using [Fc][BAr$^F{}_4$].* A mixture of **1** (10 mg, 0.022 mmol) and [Fc][BAr$^F{}_4$] (46 mg, 0.044 mmol) were dissolved in d_5-pyridine (0.5 mL) to give a dark blue solution that rapidly turns yellow. The product was analysed *in situ* by NMR spectroscopy. ^{1}H NMR (d_5-pyridine, 298 K, 400.17 MHz) δ (ppm) 8.43 (m, 16H; BAr$^F{}_4$-CH), 7.83 (m, 8H; BAr$^F{}_4$-CH), 7.68 (m, 2H; ONO-CH), 7.33 (m, 2H; (m, 2H; ONO-CH), 1.67 (s, 18H; ^{t}Bu), 1.29 (s, 18H; ^{t}Bu). ^{31}P NMR (d_5-pyridine, 298 K, 161.99 MHz): δ (ppm) −102.2 (s).

*Synthesis of [P(ONO)(μ^2-O)(μ^2:κ^1,κ^2-ONO)P] (**11**).* From an incomplete oxidation reaction (*vide infra*) an impure sample of **11** was isolated. Crystals were obtained from a hexane solution at –30 °C. ^{1}H NMR (C_6D_6, 298 K, 400.16 MHz): δ (ppm) 7.84 (m, 1H; CH), 7.81 (m, 1H; CH), 7.44 (m, 1H; CH), 7.37 (m, 1H; CH), 7.18–7.15 (m, 3H; CH), 6.6 (d, $^4J_{H–P}$ = 1.8 Hz; CH), 1.58 (s, 9H; ^{t}Bu), 1.37 (s, 18H; ^{t}Bu), 1.36 (s, 9H; ^{t}Bu), 1.28 (s, 18H; ^{t}Bu), 1.21 (s, 9H; ^{t}Bu), 1.19 (s, 9H; ^{t}Bu). ^{31}P NMR (C_6D_6, 298 K, 161.99 MHz): δ (ppm) 119.4 (d, $^2J_{P–P}$ = 31 Hz), –46.7 (d, $^2J_{P–P}$ = 31 Hz). ^{31}P{^{1}H} NMR (C_6D_6, 298 K, 161.99 MHz): δ (ppm) 119.4

(d, $^{2}J_{P–P}$ = 31 Hz), –46.7 (d, $^{2}J_{P–P}$ = 31 Hz).

*[P(ONO)(μ^2-O)(μ^2:κ^1,κ^2-ONO)P(O)] (**12**).* Compound **1** (200 mg, 0.441 mmol) was dissolved in benzene (10 mL) in an air-tight ampoule. The sample was freeze-pump-thaw degassed three times. The ampoule was placed under 1.5 atmospheres of oxygen gas and was shaken vigorously. Over time the colourless solution slowly turned dark purple. The solution was heated at 70 °C for 2 weeks giving a dark purple solution with a purple precipitate. All volatiles were removed *in vacuo* and the resultant residue was dissolved in toluene and filtered to give a purple solution. The toluene was removed under a dynamic vacuum affording crude **10** as a purple residue. Crystals were obtained from a hexane solution at –30 °C. ^{1}H NMR (C_6D_6, 298 K, 500.30 MHz): δ (ppm) 7.81 (s br, 1H; Ar-CH), 7.78 (s br, 1H; Ar CH), 7.48 (s br, 1H; Ar-CH), 7.40 (d, $^{4}J_{H–H}$ = 2 Hz, 1H; Ar-CH), 7.23 (s br, 1H; Ar CH), 7.19 (s br, 1H; Ar-CH), 7.05 (d, $^{4}J_{H–H}$ = 1 Hz, 1H; Ar-CH), 6.48 (s br, 1H; Ar CH), 1.41 (s, 9H; ^{t}Bu), 1.37 (s, 9H; ^{t}Bu), 1.35 (s, 9H; ^{t}Bu), 1.34 (s, 9H; ^{t}Bu), 1.32 (s, 9H; ^{t}Bu), 1.28 (s, 9H; ^{t}Bu), 1.21 (s, 9H; ^{t}Bu), 1.15 (s, 9H; ^{t}Bu). ^{31}P NMR (C_6D_6, 298 K, 161.99 MHz): δ (ppm) 0.4 (d, $^{2}J_{P–P}$ = 25 Hz), –45.8 (d, $^{2}J_{P–P}$ = 25 Hz). ^{31}P{^{1}H} NMR (C_6D_6, 298 K, 161.99 MHz): δ (ppm) 0.4 (d, $^{2}J_{P–P}$ = 25 Hz), –45.8 (d, $^{2}J_{P–P}$ = 25 Hz). ^{13}C{^{1}H} NMR (C_6D_6, 298 K, 125.81 MHz): δ (ppm) 149.1 (d, $J_{C–P}$ = 2 Hz; Ar-C), 149.0 (d, $J_{C–P}$ = 1 Hz; Ar-C), 148.7 (d, $J_{C–P}$ = 3 Hz; Ar-C), 147.2 (s; Ar-C), 144.3 (s; Ar-C), 144.1 (s; Ar-C), 141.9 (d, $J_{C–P}$ = 6 Hz; Ar-C), 140.5 (s; Ar-C), 140.2 (d, $J_{C–P}$ = 3 Hz; Ar-C), 139.5 (s; Ar-C), 137.6 (d, $J_{C–P}$ = 18 Hz; Ar-C), 135.5 (d, $J_{C–P}$ = 8 Hz; Ar-C), 134.3 (d, $J_{C–P}$ = 9 Hz; Ar-C), 133.4 (d, $J_{C–P}$ = 12 Hz; Ar-C), 127.9 (d, $J_{C–P}$ = 24 Hz; Ar-C), 127.7 (d, $J_{C–P}$ = 26 Hz; Ar-C), 126.7 (m br; Ar-CH), 125.1 (s; Ar-CH), 118.2 (s; Ar-CH), 117.0 (s; Ar-CH), 116.4 (s; Ar-CH), 107.1 (d, $^{3}J_{C–P}$ = 3 Hz; Ar-CH), 127.0 (d, $J_{C–P}$ = 3 Hz; Ar-CH), 106.5 (d, $J_{C–P}$ = 9 Hz; Ar-CH), 35.8 (s; ^{t}Bu-C), 35.4 (s; ^{t}Bu-C), 35.3 (s; ^{t}Bu-C), 35.3 (s; ^{t}Bu-C), 35.3 (s; ^{t}Bu-C), 35.0 (s; ^{t}Bu-C), 34.9 (s; ^{t}Bu-C), 34.9

(s; ^{t}Bu-C), 32.2 (s; ^{t}Bu-CH_3), 32.2 (s; ^{t}Bu-CH_3), 31.9 (s, two overlapping resonances; ^{t}Bu-CH_3), 31.0 (s; ^{t}Bu-CH_3), 30.4 (s; ^{t}Bu-CH_3), 30.2 (s; ^{t}Bu-CH_3), 30.1 (s; ^{t}Bu-CH_3).

*Synthesis of [K(2,2,2-crypt)]$_2$[{P(ONO)}$_2$] ([K(2,2,2-crypt)]$_2$[**13**]).* A mixture of **1** (100 mg, 0.220 mmol) and KC_8 (30 mg, 0.220 mmol) were loaded into an ampoule fitted with a gas tight valve and THF (2 mL) was added affording a yellow solution. The mixture was stirred for two hours and the solution was then filtered into a second ampoule containing 2,2,2-crypt (83 mg, 0.220 mmol). All volatiles were removed *in vacuo*, leaving an orange residue. THF (1 mL) was added to the residue, resulting in the formation of a yellow solid, which was gently heated into solution. Upon standing at room temperature, large yellow block crystals formed. After two days these were isolated by filtration and dried in vacuo. Yield: 72 mg (35%). Anal. Calcd for $C_{46}H_{76}KN_3O_8P$ (868.64 g mol^{-1}): C 63.56, H 8.81, N 4.83; Found: C 62.98, H 8.69, N 4.75. ^{1}H NMR (d_8-THF, 298 K, 400.17 MHz): δ (ppm) 7.30 (d, $^4J_{H–H}$ = 2 Hz, 1H; Ar-CH), 6.97 (d, $^4J_{H–H}$ = 2 Hz, 1H; Ar-CH), 6.36 (d, $^4J_{H–H}$ = 2 Hz, 1H; Ar-CH), 6.12 (d, $^4J_{H–H}$ = 2 Hz, 1H; Ar-CH), 3.39 (s, 12H; 2,2,2-crypt), 3.38–3.34 (m, 12H; 2,2,2-crypt), 2.39–2.34 (m, 12H; 2,2,2-crypt), 1.52 (s, 9H; ^{t}Bu), 1.31 (s, 9H; ^{t}Bu), 1.23 (s, 9H; ^{t}Bu), 0.93 (s, 9H; ^{t}Bu). ^{31}P NMR (d_8-THF, 298 K, 161.99 MHz): δ (ppm) 90.7 (s). ^{31}P{^{1}H} NMR (d_8-THF, 298 K, 161.99 MHz): δ (ppm) 90.7 (s). ^{13}C{^{1}H} NMR (d_8-THF, 298 K, 100.63 MHz): δ (ppm) 155.8 (m; Ar-C), 155.1 (s; Ar-C), 138.5 (m; Ar-C), 137.5 (s; Ar-C), 133.1 (s; Ar-C), 131.8 (s; Ar-C), 127.5 (m, s; Ar-C), 127.2 (m; Ar-C), 111.3 (s; Ar-CH), 109.9 (s; Ar-CH), 105.7(s; Ar-CH) , 104.9 (s; Ar-CH), 71.0 (s; 2,2,2-crypt), 68.3 (s; 2,2,2-crypt), 54.6 (s; 2,2,2-crypt), 35.1 (s; ^{t}Bu-C), 34.9 (s; ^{t}Bu-C), 34.8 (s; ^{t}Bu-C), 34.6 (s; ^{t}Bu-C), 32.9 (s; ^{t}Bu-CH_3), 32.8 (s; ^{t}Bu-CH_3), 30.9 (s; ^{t}Bu-CH_3), 30.7 (s; ^{t}Bu-CH_3).

*Synthesis of P(ONO)(TEMPO)$_2$ (**14**).* A mixture of **1** (100 mg, 0.220 mmol) and TEMPO (69

mg, 0.441) were added to a Schlenk tube and dissolved in toluene. The orange colour of the radical rapidly disappears leaving a colourless solution, which was stirred for 30 minutes. All volatiles were removed *in vacuo* and the residue was extracted into hexane and filtered via cannula. The resulting solution was concentrated and then cooled to −30 °C, yielding large colourless crystals, which were isolated by filtration. Yield:123 mg (73%). Anal. Calcd for $C_{46}H_{76}N_3O_4P{\cdot}C_6H_{14}$ (851.67 g mol^{-1}): C 73.28, H 10.64, N 4.93; Found: C 73.54, H 10.54, N 5.32. ^{1}H NMR (d_8-tol, 298 K, 499.93 MHz): δ (ppm) 8.01 (s, 2H; Ar-CH), 7.34 (s, 2H; Ar-CH), 2.25–0.46 (br m, 18H; TEMPO), 1.74 (s, 18H, ^{t}Bu), 1.41 (s, 18H, ^{t}Bu). ^{1}H NMR (d_8-tol, 223 K, 400.17 MHz): δ (ppm) 7.94 (s, 2H; Ar-CH), 7.30 (s, 2H; Ar-CH), 2.25–0.46 (br m, 18H; TEMPO), 1.79 (s, 18H, ^{t}Bu), 1.43 (s, 18H, ^{t}Bu). ^{31}P (C_6D_6, 298 K, 161.99 MHz): δ (ppm) −29.8 (s). ^{13}C{^{1}H} (C_6D_6, 298 K, 100.62 MHz): δ (ppm) 142.4 (Ar-C), 142.0 (Ar-C), 132.4 (Ar-C), 128.8 (Ar-C), 115.7 (Ar-CH), 105.9 (d, J_{C-P} = 14 Hz; Ar-CH), 61.2 (d, J_{C-P} = 4 Hz, TEMPO-C$(CH_3)_2$), 40.5 (br; TEMPO-CH_2), 35.0 (^{t}Bu-C), 34.9 (^{t}Bu-C), 32.1 (^{t}Bu-CH_3) 31.8 (br; TEMPO-CH_2), 29.9 (^{t}Bu-CH_3), 20.7 (br; TEMPO-CH_3).

Characterisation techniques: Single crystal X-ray diffraction data were collected using an Oxford Diffraction Supernova dual-source diffractometer equipped with a 135 mm Atlas CCD area detector. Crystals were selected under Paratone-N oil, mounted on micromount loops and quench-cooled using an Oxford Cryosystems open flow N_2 cooling device.[29] Data were collected at 150 K using mirror monochromated Cu Kα radiation (λ = 1.5418 Å; Oxford Diffraction Supernova). Data were processed using the CrysAlisPro package, including unit cell parameter refinement and inter-frame scaling (which was carried out using SCALE3 ABSPACK within CrysAlisPro).[30] Structures were subsequently solved using direct methods or using the charge flipping algorithm as implemented in the program SUPERFLIP,[31] and refined on F^2 using the SHELXL 2013-4 package.[32]

NMR samples were prepared inside a glovebox under nitrogen in NMR tubes equipped with a gas-tight valve. ^{1}H, $^{13}C\{^{1}H\}$, ^{19}F, ^{31}P NMR spectra were acquired on a Bruker AVII or AVIII NMR spectrometer at 298 K unless otherwise stated. ^{1}H and $^{13}C\{^{1}H\}$ spectra are reported relative to tetramethylsilane (TMS) and were referenced to the most downfield residual solvent resonance (C_6D_6: δ_H 7.16 ppm, δ_C 128.06 ppm; CD_2Cl_2: δ_H 5.32 ppm, δ_C 53.8 ppm; d_5-pyridine: δ_H 8.74 ppm, δ_C 150.35 ppm; d_8-THF: δ_H 3.58 ppm, δ_C 67.6 ppm; d_8-toluene: δ_H 7.09 ppm, δ_C 137.48 ppm). ^{19}F, ^{31}P NMR spectra were externally referenced to $CFCl_3$ and an 85% solution of H_3PO_4 in H_2O.

Positive ion mode electrospray mass spectra were recorded on a Bruker MicrOTOF mass spectrometer. The samples (10–20 μM) were prepared inside a glovebox under argon and the sample injected through a standard PEEK tubing feedthrough directly to the mass analyser at 10 μL min^{-1}.[33]

Elemental analyses were performed by Elemental Microanalysis Ltd, Devon. 10–15 mg samples were sent in sealed, evacuated Pyrex ampoules.

5. Acknowledgements

We thank the EPSRC (EP/K039954/1) and the SCG Innovation Fund for financial support. We also acknowledge the University of Oxford for access to Advanced Research Computing (*http://dx.doi.org/10.5281/zenodo.22558*) and Chemical Crystallography facilities, and Elemental Microanalysis Ltd. (Devon) for elemental analyses.

6. Electronic Supplementary Information

CCDC 1560356–1560368 contain the supplementary crystallographic data for this paper (www.ccdc.cam.ac.uk/data_request/cif). Experimental details, NMR spectra, ESI-MS spectra and computational details are also available.

7. References

[1] Arduengo III, A. J.; Stewart, C. A.; Davidson, F.; Dixon, D. A.; Becker, J. Y.; Culley, S. A.; Mizen, M. B. *J. Am. Chem. Soc.* **1987**, *109*, 627–647.

[2] McCarthy, S. M.; Lin, Y.-C.; Devarajan, D.; Chang, J. W.; Yennawar, H. P.; Rioux, R. M.; Ess, D. H.; Radosevich, A. T. *J. Am. Chem. Soc.* **2014**, *136*, 4640–4650.

[3] Dunn, N. L.; Ha, M.; Radosevich, A. T. *J. Am. Chem. Soc.* **2012**, *134*, 11330–11333.

[4] Zhao, W.; McCarthy, S. M.; Lai, T. Y.; Yennawar, H. P.; Radosevich, A. T. *J. Am. Chem. Soc.* **2014**, *136*, 17634−17644.

[5] Cui, J.; Li, Y.; Ganguly, R.; Inthirarajah, A.; Hirao, H.; Kinjo, R. *J. Am. Chem. Soc.* **2014**, *136*, 16764−16767.

[6] Robinson, T. P.; De Rosa, D. M.; Aldridge, S.; Goicoechea, J. M. *Angew. Chem. Int. Ed.* **2015**, *54*, 13758–13763.

[7] Cui, J.; Li, Y.; Ganguly, R.; Kinjo, R. *Chem. Eur. J.* **2016**, *22*, 9976 – 9985.

[8] Robinson, T. P.; Lo, S. K.; De Rosa, D.; Aldridge, S.; Goicoechea, J. M. *Chem. Eur. J.* **2016**, 22, 15712–15724.

[9] Zeng, G.; Maeda, S.; Taketsugu, T.; Sakaki S. *Angew. Chem. Int. Ed.* **2014**, *53*, 4633–4637.

[10] Pal A.; Vanka, K. *Inorg. Chem.* **2016**, *55*, 558–565.

[11] For recent reviews see: (a) Stephan, D. W.; Erker, G. *Angew. Chem. Int. Ed.* **2015**, *54*, 6400–6441. (b) Power, P. P. *Chem. Rec.* **2012**, *12*, 238–255. (c) Mandal, S. K.; Roesky, H.

W. *Acc. Chem. Res.* **2012**, *45*, 298–307. (d) Power, P. P. *Acc. Chem. Res.* **2011**, *44*, 627–637. (e) Asay, M.; Jones, C.; Driess, M. *Chem. Rev.* **2011**, *111*, 354–396. (f) Yao, S.; Xiong, Y.; Driess, M. *Organometallics* **2011**, *30*, 1748–1767. (g) Martin, D.; Soleilhavoup, M.; Bertrand, G. *Chem. Sci.* **2011**, *2*, 389–399. (h) Power, P. P. *Nature* **2010**, *463*, 171–177. (i) Stephan, D. W.; Erker, G. *Angew. Chem. Int. Ed.* **2010**, *49*, 46–76.

[12] Frey, G. D.; Lavallo, V.; Donnadieu, B.; Schoeller, W. W.; Bertrand, G. *Science* **2007**, *316*, 439–441.

[13] Zhu, Z.; Wang, X.; Peng, Y.; Lei, H.; Fettinger, J. C.; Rivard, E.; Power, P. P. *Angew. Chem. Int. Ed.* **2009**, *48*, 2031–2034.

[14] (a) Spikes, G. H.; Fettinger, J. C.; Power, P. P. *J. Am. Chem. Soc.* **2005**, *127*, 12232–12233. (b) Peng, Y.; Brynda, M.; Ellis, B. D.; Fettinger, J. C.; Rivard, E.; Power, P. P. *Chem. Commun.* **2008**, 6042–6044. (c) Peng, Y.; Ellis, B. D.; Wang, X.; Power, P. P. *J. Am. Chem. Soc.* **2008**, *130*, 12268–12269. (d) Peng, Y.; Guo, J.-D.; Ellis, B. D.; Zhu, Z.; Fettinger, J. C.; Nagase, S.; Power, P. P. *J. Am. Chem. Soc.* **2009**, *131*, 16272–16282. (e) Protchenko, A. V.; Birjkumar, K. H.; Dange, D.; Schwarz, A. D.; Vidovic, D.; Jones, C.; Kaltsoyannis, N.; Mountford, P.; Aldridge, S. *J. Am. Chem. Soc.* **2012**, *134*, 6500–6502.

[15] Welch, G. C.; San Juan, R. R.; Masuda, J. D.; Stephan, D. W. *Science* **2006**, *314*, 1124–1126.

[16] (a) Chase, P. A.; Welch, G. C.; Jurca, T.; Stephan, D. W. *Angew. Chem. Int. Ed.* **2007**, *46*, 8050–8053. (b) Chen, D.; Wang, Y.; Klankermayer, J. *Angew. Chem. Int. Ed.* **2010**, *49*, 9475–9478. (c) Greb, L.; Oña-Burgos, P.; Schirmer, B.; Grimme, S.; Stephan, D. W.; Paradies, J. *Angew. Chem. Int. Ed.* **2012**, *51*, 10164–10168. (d) Chernichenko, K.; Madarász, Á.; Pápai, I.; Nieger, M.; Leskelä, M.; Repo, T. *Nat. Chem.* **2013**, *5*, 718–723. (e) Mahdi, T.; Stephan, D. W. *Angew. Chem. Int. Ed.* **2013**, *52*, 12418–12421. (f) Hadlington, T. J.; Hermann, M.; Frenking, G.; Jones, C. *J. Am. Chem. Soc.* **2014**, *136*, 3028−3031.

[17] Girgis, A.; Balch, A. L. *Inorg. Chem.* **1975**, *14*, 2724–2727.

[18] Camacho-Camacho, C.; Martínez-Martínez, F. J.; Rosales-Hoz M. J.; Contreras, R. *Phosphorus, Sulfur Silicon Relat. Elem.* **1994**, *91*, 189–203.

[19] Pistner, A. J.; Moon, H. W.; Silakov, A.; Yennawar, H. P.; Radosevich, A. T. *Inorg. Chem.* **2017**, *56*, 8661–8668.

[20] Arduengo III, A. J.; Becker, J.; Davidson, F.; Kline, M. *Heterat. Chem.* **1993**, *4*, 213–221.

[21] Addison, A. W.; Rao, T. N.; Reedijk, J.; van Rijn, J.; Verschoor, G. C. *J. Chem. Soc., Dalton Trans.* **1984**, 1349–1356.

[22] (a) Godfrey, S. M.; McAuliffe, C. A.; Mushtaq, I.; Pritchard, R. G.; Sheffield, J. M.; *J. Chem. Soc. Dalton Trans*. **1998**, 3815–3818. (b) Burford, N.; Clyburne, J. A. C.; Gates, D. P.; Schriver, M. J.; Richardson, J. F. *J. Chem. Soc. Dalton Trans.* **1994**, 997–1001.

[23] (a) Cotton, A.; Kibala, P. A. *J. Am. Chem. Soc.* **1987**, *109*, 3308–3312. (b) Núñez, R.; Teixidor, F.; Kivekäs, R.; Sillanpää, R.; Viñas, C.; *Dalton Trans.* **2008**, 1471–1480. (c) Godfrey, S. M.; Kelly, D. G.; McAuliffe, C. A.; Mackie, A. G.; Pritchard, R. G.; Watson, S. M. *J. Chem. Soc. Chem. Commun.* **1991**, 1163–1164. (d) Barnes, N. A.; Flower, K. R.; Godfrey, S. M.; Hurst, P. A.; Khan, R. Z.; Pritchard, R. G. *Cryst Eng Comm* **2010**, *12*, 4240–4251. (e) Dillon, K. B.; Waddington, R. C. *Nature Physical Science*, **1971**, *12*, 158–159.

[24] (a) Ruban, A.; Nieger, M.; Niecke, E. *Angew. Chem. Int. Ed. Engl.* **1993**, *32*, 1419–1420. (b) Ruban, A.; Nieger, M.; Niecke, E. *Eur. J. Inog. Chem.* **1998**, 83–85.

[25] Pyykkö, P.; Atsumi, M. *Chem. Eur. J.* **2009**, *15*, 186–197.

[26] (a) Larsen, S. K.; Pierpont, C. G. *J. Am. Chem. Soc.* **1988**, *110*, 1827–1832; (b) Simpson, C. L.; Boone, S. R.; Pierpont, C. G. *Inorg. Chem.* **1989**, *28*, 4379–4385; (c) Bruni, S.; Caneschi, A; Cariati, F.; Delfs, C.; Dei, A.; Gatteschi, D. *J. Am. Chem. Soc.* **1994**, *116*, 1388–1394; (d) Chaudhuri, P.; Hess, M.; Weyhermüller, T.; Wieghardt, K. *Angew. Chem.*

Int. Ed. **1999**, *38*, 1095–1098; (e) Zarkesh, R. A.; Ziller, J. W.; Heyduk, A. F. *Angew. Chem. Int. Ed.* **2008**, *47*, 4715–4718; (f) Hananouchi, S.; Krull, B. T.; Ziller, J. W.; Furche, F.; Heyduk, A. F. *Dalton Trans.* **2014**, *43*, 17991–18000.

[27] Yonekuta, Y.; Oyaizu, K.; Nishide, H. *Chem. Lett.* **2007**, *36*, 866–867.

[28] Chávez, I.; Alvarez-Carena, A.; Molins, E.; Roig, A.; Maniukiewicz, W.; Arancibia, A.; Arancibia, V.; Brand, H.; Manríquez, J. M. *J. Organomet. Chem.* **2000**, *601*, 126–132.

[29] Cosier, J.; Glazer, A. M. *J. Appl. Cryst.* **1986**, *19*, 105–107.

[30] CrysAlisPro, Agilent Technologies, Version 1.171.35.21.

[31] Palatinus, L.; Chapuis, G. *J. Appl. Cryst.* **2007**, *40*, 786–790.

[32] a) Sheldrick, G. M. *Acta Cryst.* **2008**, A64, 112–122; b) Sheldrick, G. M. *Acta Cryst.* **1990**, A46, 467–473; c) SHELX2013, Programs for Crystal Structure Analysis (Release 2013), Sheldrick, G. M., University of Göttingen (Germany), 1998.

[33] Lubben, A. T.; McIndoe, J. S.; Weller, A. S. *Organometallics* **2008**, *27*, 3303–3306.

TOC